Material recovery from waste polyethylene terephthalate (PET)

Laura S Diaz-Silvarrey[a,*], Andrew McMahon[a], Anh N. Phan[a,**]

[a]School of Engineering, Newcastle University, Newcastle upon Tyne

Abstract

Polyethylene terephthalate (PET) is one of the main plastics used in food packaging products, which have a very short life and are rapidly transformed into waste, and accounts for 7wt% of the total plastic waste generated. Current PET waste management, mainly via mechanical recycling and glycolysis, have encountered a number of issues: negative impact on the environment, segregation of waste and product separation/purification. Therefore other versatile alternatives such as pyrolysis should be employed to recover value-added products from waste. Benzoic acid a precursor in the food and beverage industry, derived from PET via thermochemical conversion opposed to the current manufacturing process from fossil fuel-based feedstock is considered as a promising approach. In this study, the effect of operating conditions i.e. temperature, catalyst to plastic mass ratio and volatiles residence time and their interactions on product yields and properties were studied. Sulphated zirconia (SZ) was first time used for catalytic pyrolysis of PET due to its high acidity and environmentally friendly synthesis. Results showed that up to 27-32wt% benzoic acid could be recovered through PET pyrolysis at 450-600^oC at 20s residence time. By increasing the catalyst:plastic ratio to 10wt% only 26wt% of benzoic acid was recovered in the wax but it increased the amount of other valuable products i.e. light hydrocarbons (C_1-C_3) recovered in the gas.

Keywords: PET, plastic waste, pyrolysis, catalysis, sulphated zirconia

1. Introduction

Commodity plastics i.e. polyethylene terephthalate (PET), polystyrene (PS), polypropylene (PP), polyethylene (PE), polyvinyl-chloride (PVC), which are produced from petroleum-based products, have been widely used due to their versatility, durability, low weight and cost [1, 2]. This causes an increase in waste i.e. average 8.7% per year [3]. The current depletion of petroleum resources coupled with the growing concern of plastic waste and their damaging effect on the Environment and ecological systems, recovery of monomers from plastic waste is now more imperative than it has ever been.

In the European Union (EU), and in the UK, it is estimated that plastic waste contributes up to 10-13% of municipal solid waste (MSW) [4, 5], of which 7wt% (1.7 million tonnes) is PET [1]. PET is widely used in the textile and carpet industry, in the packaging of food products and in the production of bottles

*l.diaz-silvarrey@newcastle.ac.uk
**anh.phan@newcastle.ac.uk

[6, 7]. PET waste is usually managed by landfill disposal, chemical recycling (methanolysis, glycolysis, hydrolysis), energy recovery via incineration and mechanical recycling. Themelis and Mussche [2] reported that approximately 83 % of plastic waste was disposed in landfills while only 7 % was recycled and 10 % was converted into energy via waste-to-energy plants in the USA in 2014. Although recycling and recovery rates were higher in the EU in the same year (30 %), still around 31 % of plastic waste was disposed in landfills with the balance converted into energy via waste-to-energy plants [1]. However, due to lack of recycling capacity plastic waste used to be sent to China for treatment. For instance, from the almost 600 ktonnes of plastic waste recycled in 2009 in the UK about 75 % were shipped abroad [8]. Since the beginning of 2018, the Chinese Government implemented a ban to import plastic waste which has led to an accumulation of plastic waste in the UK [9] that require versatile and alternative management solutions.

Since plastic waste are non-biodegradable, their disposal in landfills causes a negative impact on ecology, human health and wildlife [10]. Incineration with energy recovery, a common approach that reduces considerably the volume of wastes and produces energy, also emits airborne pollutants such as CO_2, N_2O, NOx, NH_3, VOC, polychlorinated dibenzo-p-dioxins and dibenzofurans (PCDD/PCDF), HCl, HF and SO_2 [11–15]. Mechanical recycling of PET, done by melting and extrusion of PET wastes into fibres, produces products with limited applications e.g. drinking bottles and food-graded materials require the use of virgin PET manufactured from fossil fuels. Therefore, from a sustainable point of view, chemical recycling via glycolysis or pyrolysis is preferred as an alternative to recover of raw materials.

Glycolysis is the common PET chemical recycling method to recover bis(hydroxyethyl) terephthalate (BHTE) monomer. It is the depolymerisation of PET through the solvolytic chain cleavage into smaller molecules in the presence of ethylene glycol at temperature and pressure ranges of 190-240 ^{o}C and 0.1-0.6 MPa over a long reaction time (0.5-8 h) [16]. In addition, this process requires a basic catalyst to obtain a reasonable yield of BHTE i.e. 6-70 % [17] at milder conditions [18]. Most catalysts are liquids in the form of metal acetates [17, 19], titanium-phosphates [17], solid super acids [17], metal oxides [17], ionic liquids[19], hydrotalcites [19], or enzymes [19]. The main disadvantages of PET glycolysis are i) the requirement of clean and pure PET waste streams, therefore requiring high segregation costs [6, 11, 12]; ii) the use of liquid catalysts that required further separation from glycolysis products creating waste water that requires treatment; and iii) the catalysts cannot be reused after separation increasing operation costs. Further details can be found elsewhere [16, 18, 20] but will not be discussed here as they escape the scope of this work.

Pyrolysis is an advanced thermochemical conversion carried out in a non-oxidant atmosphere at temperatures between 400-700 ^{o}C with or without a catalyst. Pyrolysis of plastic waste yields three fractions: solid residue, formed by carbon residue and any inorganic element present in the original plastic product; gas, comprised of CH_4, H_2, CO_2, CO and C_2-C_5 hydrocarbons; and wax/liquid/oil which comprises of a mixture of aliphatic and aromatic hydrocarbons. Pyrolysis can be applied to recover valuable chemicals from PET without cleaning, waste segregation [1, 6], the use of liquid catalysts and extra reagents. Unlike glycolysis, where the monomer (BHTE) is recovered, pyrolysis of PET yields other aromatic and oxygenated compounds like acetaldehyde, vinyl benzoate or benzoic acid [21] due to the difference in the decomposition mechanism. Kumagai et al. [22] showed that CaO catalyst/steam increased the amount of benzoic acid recovered in PET pyrolysis at 600 ^{o}C from 1.83 wt% to 8.29 wt%. During glycolysis, PET ester link is substituted by the hyroxyl group from the reagent glycol forming oligomers or oligoester diols/polyols with hydroxyl terminal groups being the most common one BHTE [16, 23]. Pyrolysis of PET is also produced via the cleavage of the ester linkage. However, as there are no glycols present, the bond cleavage is produced by the effect of either temperature or both temperature and catalyst resulting in the formation of vinyl ester and carboxyl compounds. The vinyl ester could decompose further into other compounds such as acetaldehyde, acetophenone or light hydrocarbons (C_1-C_3) [24].

Benzoic acid, one of the products from PET pyrolysis, is mainly used in the food and beverage industry as an intermediate to produce benazoates and other related antifungal preservatives (such as E210, E211, E212 and E213) present in numerous common foods like soft drinks, coffee, salad dressings, etc. as well as one of the main feedstock for phenol manufacture [25]. Benzoic acid is also used as a precursor of other products such as plasticizers, fungal ointments for medical use, and as a calibrating substance for bomb calorimeters [25]. Its market size is expected to increase by almost 30% in the next few years (from 480 ktons in 2014 to 620 ktons in 2023) [25] and its price is around $4000/Mton [26]. Therefore, the recovery of this compound is as important as that of the monomer BHET because benzoic acid is currently manufactured by partial oxidation of toluene with oxygen in the presence of cobalt or manganese naphthenates.

Research on pyrolysis process for different types of plastic in the plastic waste stream has been carried out over the years [21, 27–37], but only focusing on the effects of individual parameters such as the pyrolysis temperature (300K to 1000K), the type of catalyst (HZSM-5, HUSY, HMOR, Z-N, Silica-Alumina, Zeolite-Beta and SZ [38]), ratio of plastic to catalyst (100:1 to 10:1), and heating rate (5, 10 and 20K/min). The effect of temperature was also studied focusing on reactions pathways and product yields and distribution from PET pyrolysis [30, 39]. However, none of these studies looked at the synergistic effect of the pyrolysis temperature and SZ catalyst. In this study, the interactions of temperature and plastic:catalyst mass ratio on the product distribution of PET waste pyrolysis to recover valuable chemicals, i.e. benzoic acid. SZ was chosen because (i) it is a super acid catalyst [40], i.e. it activates light alkanes at room temperature [41], that is found to be effective for cracking of long chain hydrocarbons (triglycerides/vegetable oil [42, 43] and polystyrene [38]) and (ii) an environmentally friendly alternative compared to catalysts mentioned previously. However, limited research has also been carried out using SZ catalyst for pyrolysis of plastic waste, particularly for PET and examining the viability of using SZ in comparison to other common catalysts applied in the pyrolysis process of PET [31].

2. Experimental methodology

2.1. Materials

PET samples were collected from O'Brien's Waste Recycling Solutions (Wallsend, Newcastle upon Tyne, UK). They were thoroughly washed with soap and water to eliminate any effects caused by unknown contaminants, and then cut into 1.5x1.5cm size. PET waste characterisation is shown in Table 1. PET waste had a H/C ratio similar to that of lignite and lower than that of biomass [44] implying a very low hydrogen content due to the existence the aromatic rings, ester and carboxylic group as shown in Figure 1. The high calorific value of PET was similar to that of bituminous (17-23MJ/kg) or lignite coal (15-27 MJ/kg).

Table 1: PET waste characterisation

	PET waste
High calorific value / [MJ/kg]	22.860±0.005
Volatile matter / [wt%]	87.62±0.26
Ash content / [wt%]	2.39±0.64
Empirical formula	$C_5H_5O_2$

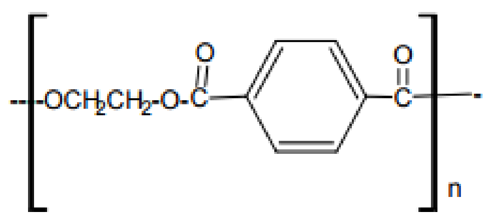

Figure 1: Structure of PET

2.2. Catalyst preparation and characterisation

SZ catalyst was synthesised by directly mixing zirconium (IV) oxychloride octahydrate (Sigma Aldrich) and ammonium sulphate (Sigma Aldrich) at 1:6 molar ratio followed by 18h ageing at constant temperature inside a VECSTAR VC1 horizontal furnace kept at 25^{o}C. The mixture was then calcined at 500^{o}C for 6h in the same furnace following the method described by Eterigho et al. [43]. The solvent free synthesis of SZ was proven to improve catalyst characteristics [45] due to a stronger interaction between SO_4^{2-} and ZrO_2 that reduces catalyst deactivation [46]. The morphology of the prepared catalyst was conducted using a Philips CM100 Transmission Electron Microscopy (TEM) with Compustage and high resolution digital image capture particle size distribution. Particle size distribution of the prepared catalyst was determined using Image J based on the TEM image shown in Figure 2. Results showed that around 60% of the particles were in the 1-2.9nm range while the rest were distributed from 2.9-4.8nm (15%), 4.8-6.7nm (10%) and 6.7-18.1nm (15%).

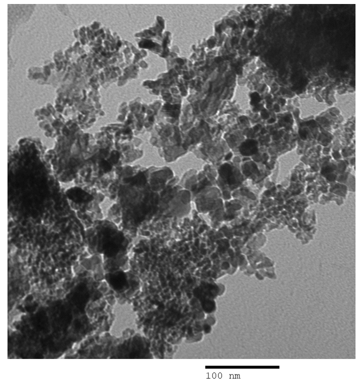

Figure 2: TEM image of SZ catalyst (180000x, HV = 100.0kV, scale = 100nm)

X-ray diffractograms (XRD) were obtained in a Panalytical X'Pert Pro Multopurpose Diffractometer (MPD) fitted with a X'Celerator and a secondary monochromator (Cu-Kα radiation, wavelength (λ) = 1.54$\mathring{A}$ generated at 40kV and 40mA) over a 2θ range of 2^o to 70^o from 2^{o}C - 100^{o}C. As shown in Figure 3, the sample was mainly amorphous with relatively low tetragonal and monoclinic phase crystalline fractions. The results were similar to those reported by Eterigho et al. [43] although the crystalline fraction of the SZ in this study was slightly higher.

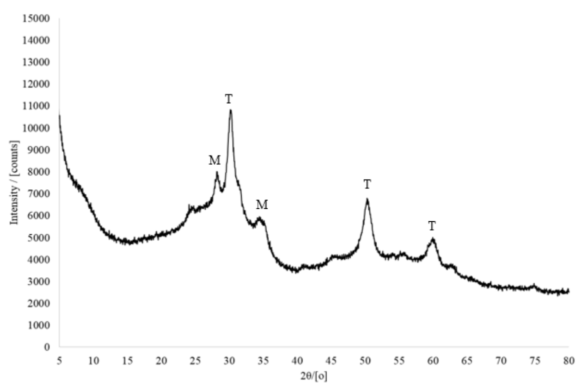

Figure 3: X-ray diffraction spectra of SZ (T = tetragonal crystal and M = monoclinic crystal)

Surface area was obtained by N_2 physisorption isotherms determined at 77K using a Thermo Scientific Surfer and Brunauer-Emmett-Teller (BET) equation with samples outgassed at 150^{o}C over high vacuum for 12h prior to analysis. SZ had a high surface area (277$\pm$15m^2/g), which was twice higher than those reported, i.e. 108m^2/g [43], 119.3m^2/g [47]. The difference could be due to the conditions used during the catalyst preparation. Hamouda et al.[48] and Stichert and Schüth [49] found that the surface area could dramatically vary from 19m^2/g (no aging) to 104m^2/g (1 day aging at 423K) [49].

2.3. Kinetic parameters

Only PET waste were cut into circular particles of 1mm diameter and analysed by thermogravimetric analysis (TGA) in a Perkin Elmer STA6000 at 5, 10, 20 and 40^{o}C/min between 30-700^{o}C to obtain kinetic parameters of PET pyrolysis using isoconversional methods as described in detail elsewhere [50]. TGA and differential TGA curves of the PET waste sample and its kinetic parameters (activation energy, pre-exponential factor and order of reaction) are illustrated in Figure 4 and Table 2 respectively. Figure 5 shows the variation of the waste PET heat flow during TGA analysis as temperature increased.

Table 2: Results of kinetic analysis [50]

	PET waste
Decomposition temperature range / [^{o}C]	395-520
Activation energy / [kJ/mol]	197.61
Order of reaction	2.8

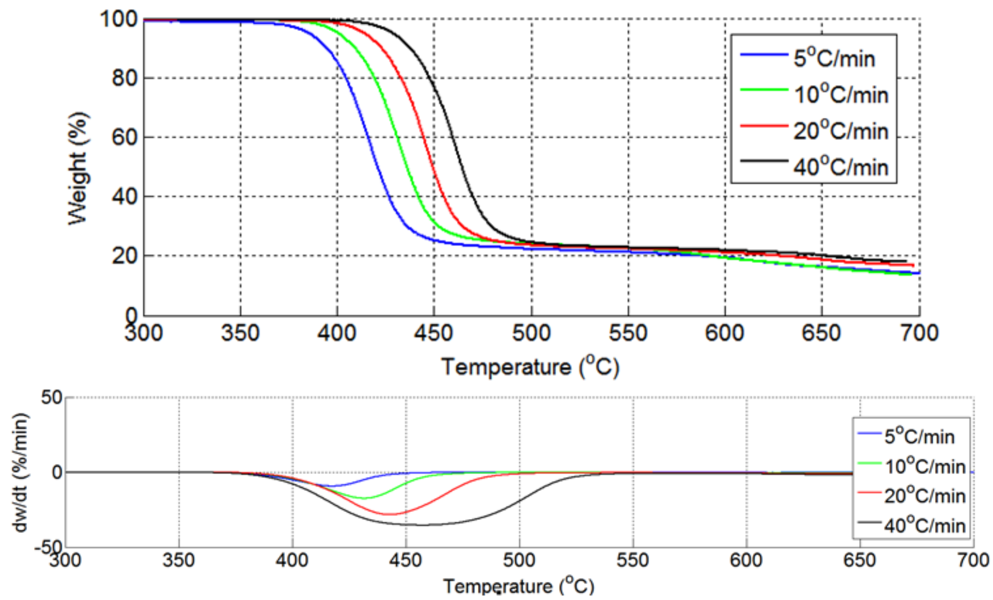

Figure 4: TGA (top) and differential TGA (bottom) curves for PET samples obtain at 5^{o}C/min, 10^{o}C/min, 20^{o}C/min and 40^{o}C/min between 300-700^{o}C

From TGA analysis (Figure 4), it can be observed that PET decomposition started at around 395 ^{o}C and completed about 520 ^{o}C. Figure 5 shows a perturbation on the heat flow after PET decomposition temperature at high heating rates (> 20 ^{o}C/min) that is not perceptible at low heating rates (< 20 ^{o}C/min). This perturbation is thought to be caused by a temperature profile formed on the plastic particle caused by a decrease in the uniformity of the heat distribution at high heating rates due to the low thermal conductivity of plastics. This phenomenon prevents the PET particle to melt completely and therefore part of the thermal decomposition occurs on melted plastic i.e. liquid and part on the non-melted plastic i.e. solid. Pyrolysis temperature for the experiments was set based on the range determined by TGA. The minimum temperature selected was 450 ^{o}C to ensure over 20% PET decomposition. The maximum experimental temperature selected was 600 ^{o}C to obtain complete PET decomposition. The remaining experimental temperature was

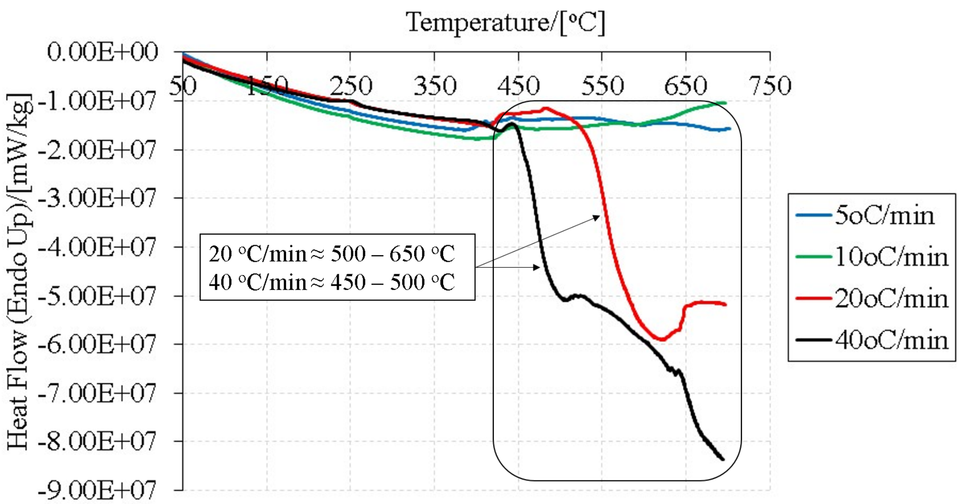

Figure 5: Heat flow (mW/kg) curves for PET samples obtain at 5^{o}C/min, 10^{o}C/min, 20^{o}C/min and 40^{o}C/min between 50-700^{o}C

selected as the medium point of the selected interval.

2.4. Pyrolysis methodology

Experimental set up for pyrolysis was shown in Figure 6. Approximately 5.04±0.03 g of PET were placed in a quartz combustion boat inside a 30 cm long and 29 mm inner diameter quartz reactor. A 10 mm long catalyst bed was created just after the sample by mixing the desired amount of the SZ catalyst (3wt%, 6.5wt% or 10wt% of the PET sample) with 10 g of 1 mm diameter glass beads (Sigma-Aldrich) in order to: i) obtain uniform distribution of the catalyst, ii) ensure uniform contact of the volatiles released from pyrolysis and the catalyst and iii) prevent the catalyst to flow out of the reactor with the volatiles to prevent wax contamination in the condenser.

The pyrolysis reactor containing the PET sample and the catalyst packed bed was placed inside a cylindrical horizontal Vecstar VCTF/SP furnace. The reactor was continuously purged with nitrogen at a flow rate of 20 mL/min for 1 h. As soon as the system was air free (confirmed by gas chromatography analysis of the gas collected at the outlet), the furnace was switched on to heat the reactor to the desired pyrolysis temperature (450, 525 or 600 ^{o}C) at 45 ^{o}C/min. Both the sample and the catalyst bed were heated at the same heating rate i.e. 45 ^{o}C/min up to the same final temperature i.e. 450, 525 or 600 ^{o}C as the furnace heated zone has an uniform horizontal temperature distribution. All temperatures given referred to the one measured at the centre of the heated zone. The heating rate given also refers to the one measured at the centre of the heating zone during the furnace calibration prior to any experiment. The temperature was held for 10 minutes from the time the sample reached its set point before the furnace was turned off to ensure full decomposition of the volatiles released. The residence time of the volatiles inside the heated zone i.e.

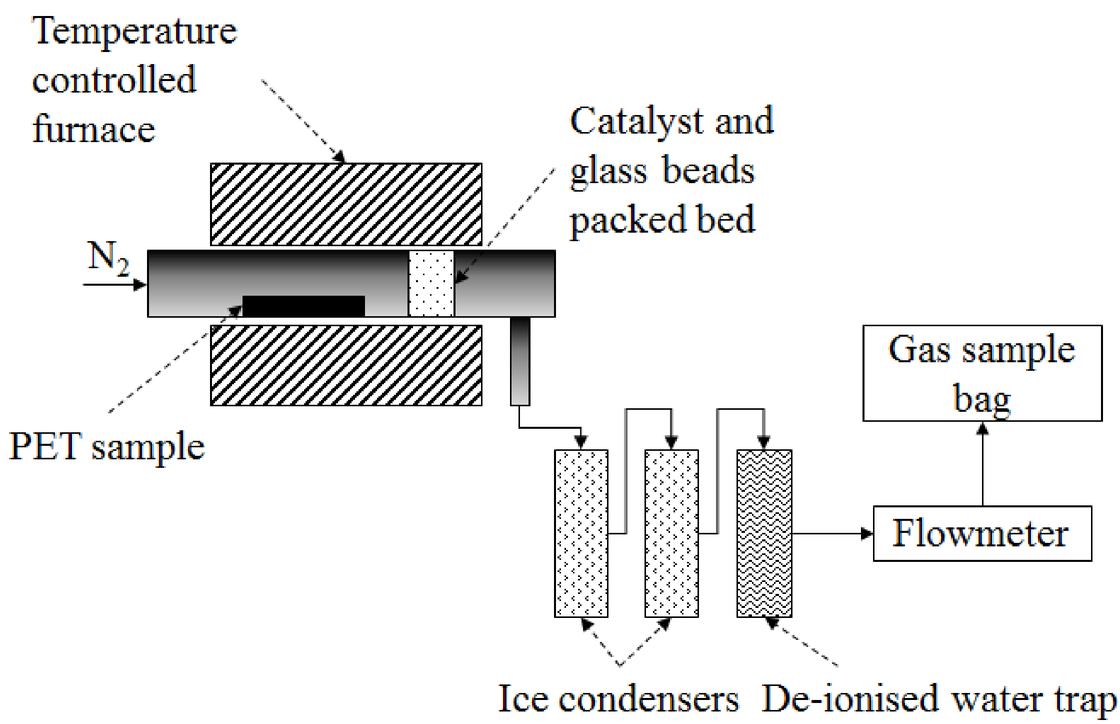

Figure 6: Experimental set up

the time the volatiles remained inside the catalyst bed in contact with the catalyst, was varied (10, 20 or 30 s) by altering the nitrogen flow rate (40 mL/min, 20 mL/min and 13 mL/min respectively).

At the outlet of the reactor, volatiles were condensed in two condensers cooled with ice (0^oC). The gases out of the condenser (non-condensable gases) were passed through a water trap to ensure no residues enter the gas collection system. A 0.6L Tedlar bag (Sigma-Aldrich) was used to collect the gas when the sample reached the final pyrolysis temperature (450^oC, 525^oC or 600^oC) for further analysis. The solid residue in the combustion boat and condensed fraction were collected and weighted for their yields once the system cooled down below 100^oC under N_2 atmosphere to minimise further decomposition of the products. The gas yield was calculated by mass balance difference as explained in equation 1. The catalyst was recovered from the catalyst bed by simple separation from the glass beads via agitation.

$$M_{PET} = M_{SolidResidue} + M_{Wax} + M_{Gas} \tag{1}$$

where M_{PET} is the initial mass of PET (g), $M_{SolidResidue}$ is the mass of solid residue in the combustion boat (g), M_{Wax} is the mass of the condensed fraction i.e. wax (g), and M_{Gas} is the mass of the non-condensable fraction i.e. gas calculated by difference (g).

The yield of the three products recovered from PET pyrolysis i.e. solid residue, wax and gas, were calculated based on the ratio between the mass recovered and the initial mass of PET, as described in equation 2.

$$Y_i = \frac{M_i}{M_{PET}} * 100 \qquad (2)$$

where i represents the products: solid residue, wax and gas, Y_i is the yield (wt%), M_i the mass of product at the end of pyrolysis (g) calculated either by weighting as explained above or by difference and M_{PET} is the initial mass of PET (g).

2.5. Product analysis

2.5.1. Gas analysis.

Gas samples were analysed by a Varian 450 gas chromatography unit equipped with (i) a TCD detector (held at 175^{o}C) and three columns: Haysep T ultimetal 0.5m x 0.3175mm, Haysep Q ultimetal 0.5m x 0.3175mm and Molsieve ultimetal 1.5m x 0.3175mm kept isothermally in an oven at 175^{o}C and (ii) an FID detector (held at 250^{o}C) coupled with a CP-Sil 5CB 25m x 0.25mm x 0.40μm in an oven programmed as follows: 40^{o}C hold for 2min, 4^{o}C/min to 50^{o}C and hold for 0.5min, 8^{o}C/min to 100^{o}C and final ramp to 120^{o}C at 10^{o}C/min. The results from GC-TCD/FID gas analysis are referred to the initial PET sample (i.e. mass of compound/mass of PET sample).

2.5.2. Wax analysis.

A known fraction of the wax sample was dissolved in n-hexane and analysed by both gas chromatography mass spectrometry (GC-MS) for qualitative analysis and gas chromatography flame ionized detector (GC-FID) for quantitative analysis. GC-MS analysis was performed in a Clarus 560D equipped with Elite-5MS 30m x 0.25mm x 0.25mm column. GC-FID analysis of the wax sample was made on an Agilent 7820N unit equipped with a CPSil5 CB 25m x 0.25mm x 0.40mm column. The method used for both GC-MS and GC-FID was as follows: temperature of the detector and inlet set at 280^{o}oC and oven programmed to start at 60^{o}C with 3min hold and then ramped to 280^{o}C at 6.5^{o}C/min followed by a 13.5min hold. Quantitative results from GC-FID were obtained based on a calibration curve with benzoic acid (99%, Alfa Aesar) at different concentrations as well as injecting 1μL of methyl heptadecanoate dissolved in n-hexane (500ppm, Sigma Aldrich) with every sample as internal standard. Results from GC-FID wax analysis are calculated based on the initial PET mass (i.e. mass of compound/mass of PET sample).

An equivalent amount of wax was also dissolved in dimethyl sulfoxide (DMSO) and analysed by proton nuclear magnetic resonance (^{1}H-NMR) to cross examine the GC-MS results. ^{1}H-NMR of the sample was conducted in a Bruker Avance III HD 700 NMR Spectrometer operating at 700.13MHz. The spectra were acquired in d6-DMSO at 298K and were referenced to TMS. The number of scans was 256. Finally, the wax as collected from the condensed was scanned from 4000-600cm^{-1o} on an Agilent Cary 630, using KBr as background reference.

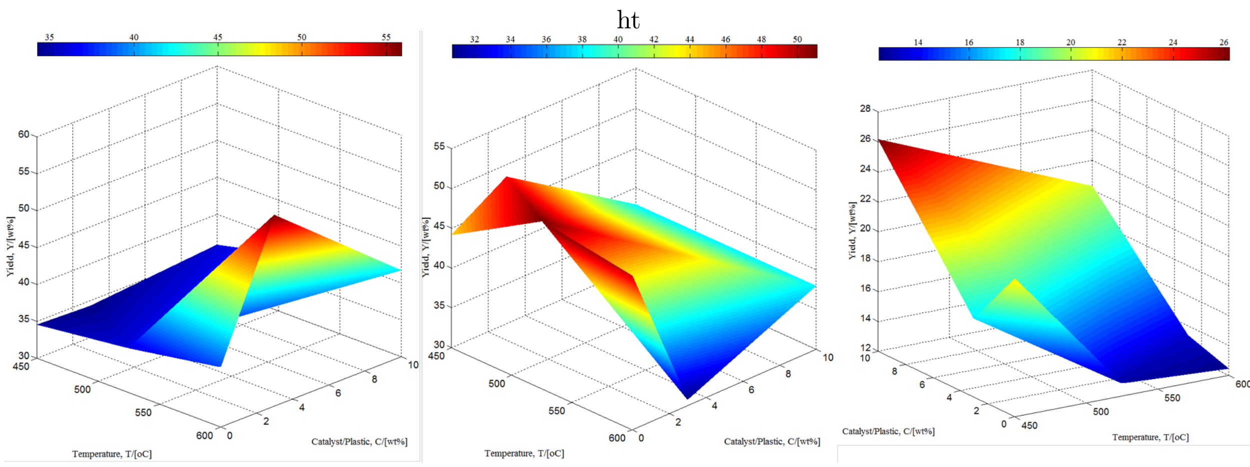

Figure 7: Effect of temperature and catalyst:plastic mass ratio on the gas yield (left), wax yield (middle) and residue yield (right) at volatile residence time of 20s. Red areas represent higher values while blue areas lower values according to the colour bar on top of each subfigure. Green and yellow areas are intermediate values.Errors: gas yield = ± 6.37 wt%, wax yield = ± 7.60 wt% and residue yield = ± 8.53 wt%

3. Results and Discussion

PET is a stiff semi crystalline polymer formed by repetition of the structure shown in Figure 1. When PET is exposed to high temperatures ($\geq$395^{o}C), it decomposes via a random scission of the ester linkage resulting in the formation of a vinyl ester and a carboxyl group (benzoic acid). The vinyl ester undergoes transesterification to form acetaldehyde and other smaller molecules such as CO, CO_2 or ethylene [24, 51]. The rate of PET decomposition and its product distribution depends on the temperature, the amount of catalyst/type of catalyst and the residence time of the volatiles [24].

3.1. Effect of operating conditions on decomposition of PET

Figure 7 shows the variation of temperature and catalyst:plastic mass ratio for the gas yield (left), the wax yield (middle) and residue yield (right). It was found that at the tested operating conditions: temperature (450-600 ^{o}C), volatile residence time in the heated zone (10-30s) and catalyst:plastic mass ratio (3-10wt%), temperature had the strongest effect on the product yield, followed by the catalyst:plastic mass ratio. Increasing temperature enhanced the production of the gas at the expense of wax fraction. At low temperature (i.e. 450 ^{o}C) increasing the catalyst proportion increased the solid residue yield but did not have a clear effect on the gas and wax yield. At high temperature (i.e. 600 ^{o}C), the gas yield maximised whereas the wax yield minimised at catalyst:plastic ratio of 2/30 (i.e.6.5 wt%). In contrast, the solid residue yield increased with catalyst (12.45 wt% with no catalyst, 13.37 wt% at 3 wt% catalyst and 20.28 wt% at 10 wt% catalyst).

As explained in section 2.4, the solid residue represented the residue recovered from the combustion boat after PET pyrolysis. Therefore this fraction was not in contact with the catalyst bed. The solid residue yield varied mainly due to differences in the composition of PET waste i.e. drink bottles, ready-meal packets, etc.

The effect of the catalyst on PET decomposition was more prominent at high temperature (600 ^oC). For example, increasing the catalyst:plastic mass ration at 450 ^oC from 0 to 1:10 (i.e. from 0 wt% to 10 wt%) resulted in a 3 % increase of the gas yield (from 34.54 wt% to 35.87 wt%) while at 600 ^oC the gas yield increased by 29 % (from 38.19 wt% to 55.91 wt%). This suggested the minimum temperature required to activate the catalyst to enhance secondary cracking is above 450 ^oC.

The volatiles residence time i.e. the time the volatiles remained inside the catalyst bed in contact with the catalyst, in the tested range of 10-30 s had little effect the product yields. This observation agreed well with the work by Mastral et al. [52] who observed that the residence time in the range of 0.81-1.45 s had no significant effect on the product distribution of plastic waste pyrolysis at temperatures below 685 ^oC. However, there is a general consensus that longer residence times of the volatiles in the reactor enhance the formation of light hydrocarbons and non-condensable gases due to secondary cracking reactions [32, 53]. Therefore, the little effect of the residence time on the product yields on this study could be due to the small range tested. The residence time could not be altered over a wider range due to experimental restrictions so the effect of reaction-space time was not further studied and will remain constant at 20 s in the discussion from this point forward.

3.2. Effect of operating conditions on the gas composition

As expected, higher temperatures promote the cracking of heavier compounds into lighter molecules, thereby increasing the gas yield and decreasing the wax yield as shown in Figure 7. As reported by Martín-Gullón et al. [30] as temperature increased, a fraction of the already formed residue was further decomposed, thereby increasing the proportion of carbon monoxide and carbon dioxide in the gas fraction. Figure 8 shows the evolution of carbon dioxide and carbon monoxide in the gas fraction with temperature and catalyst:plastic ratio.

It was found that without catalyst, increasing the temperature had little effect on CO_2 yield (19.4 wt% at 450 ^oC to 17.25 wt% at 600 ^oC) while had no effect on the yield of CO (11.5 wt% at 450 ^oC to 11.6 wt% at 600 ^oC). CO_2 yield variation was found to be corresponded to the solid residue yield due to the reverse Boudouard reaction occurring to some extent at the tested conditions to transform CO_2 into CO as shown in reaction (3). At 450 ^oC (theoretical molar fraction: CO_2 = 0.969 and CO = 0.031 [54]) the forward reaction was promoted towards the formation of CO_2 8) and solid residue 7) whereas increasing temperature to 600 ^oC (theoretical molar fraction: CO_2 = 0.723 and CO = 0.277 [54]) favoured the formation of CO (Figure 8). Figure 8 initially suggested that SZ could affect the reverse Boudouard reaction to form CO from CO_2 and solid residue. It was reported [55] that alkali and alkaline metals (i.e. Na, Ca, Mg, etc.) decreased the minimum temperature to promote the reverse Boudouard reaction from 700 ^oC to 580 ^oC. It has also been suggested that the surface oxygen in metal oxides like ZrO_2 can act as a substrate for carbon residue deposition via the Boudouard reaction (reaction (3)) at high temperatures [56]. However, no previous work was found involving SZ as a Boudouard reaction catalyst. Therefore, the CO_2 yield reduction at high temperature and high catalyst proportion is suggested to be formed via the Boudouard reaction along with

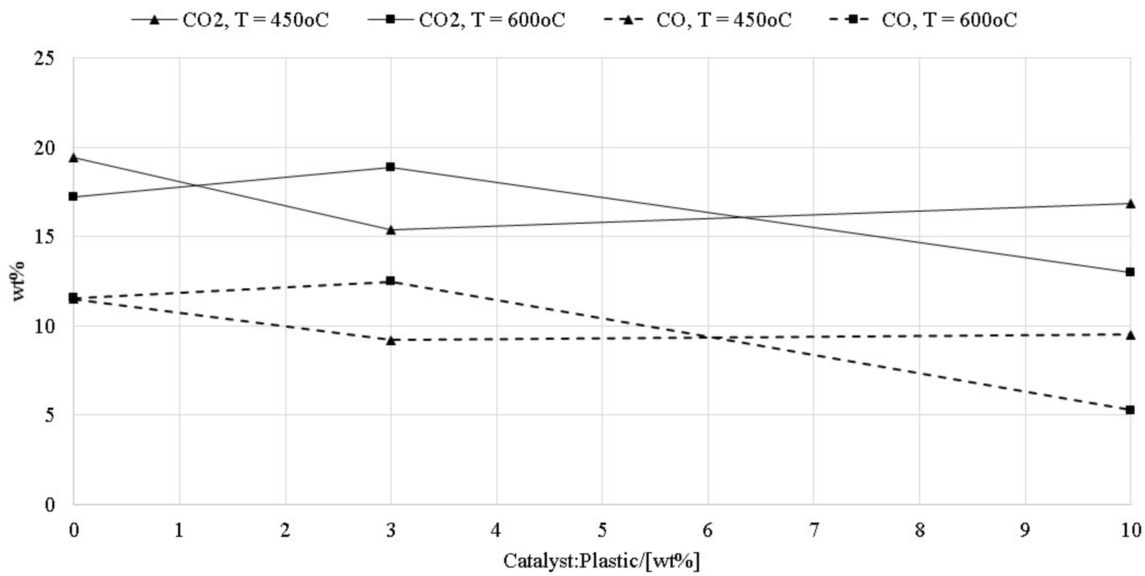

Figure 8: Effect of temperature (450-600 ^oC) and catalyst:plastic mass ratio (0-10wt%) on the yield of CO_2 (solid line, ±2.70 wt%) and CO (dashed line, ±1.86 wt%) formation in PET pyrolysis gas. Triangles represent T = 450 ^oC and squares represent T = 600 ^oC

carbon residue but consumed by methane in an oxidative coupling with CO_2 as oxidant to form other light hydrocarbons. The carbon residue deposited on SZ surface causes deactivation of the catalyst. Further work on the effect of SZ in the Boudouard reaction will be beneficial to consolidate these conclusions.

$$2CO \leftrightarrow CO_2 + C_{(s)} \tag{3}$$

Figure 9 shows the variation of the remaining gas products: H_2, O_2, CH_4 and C_2-C_5 hydrocarbons with temperature and catalyst:plastic mass ratio at constant volatiles residence time of 20s. The amount of light hydrocarbons (left figure, dashed line, triangles for 450^oC and squares for 600^oC) increased with both the catalyst:plastic mass ratio (0wt% to 10wt%) and temperature (450 ^oC to 600 ^oC). At low temperatures (450 ^oC) the amount of CO_2 and CO decreased with increasing the catalyst loading (Figure 8), leading to the formation of light hydrocarbons (C_1-C_4) and oxygen (Figure 9. At high temperatures (600 ^oC), the formation of CO_2 and CH_4 was favoured at low catalyst loads whereas the formation of light hydrocarbons and oxygen increased with the catalyst load.

SZ catalyst contained crystalline ZrO_2 providing surface oxygen which can interact with some of the reaction products such as CH_4. At high temperature (600 ^oC), a proportion of the CH_4 generated can react with CO_2 as an oxidant agent: $2CH_4 + CO_2 \rightarrow CO + C_2H_6 + H_2O$ and $C_2H_6 + CO_2 \rightarrow CO + C_2H_4 + H_2O$ [57, 58]. During this reaction oxygen is necessary to create a methyl radical intermediate (CH_3^*) which can then undergo a chain reaction mechanism to form multiple hydrocarbons i.e. C_2, C_3 and C_4. The oxygen in gas phase it can also react with CH_3^* to form further CO_2 via CH_3O_2 and CH_2O radicals mechanism.

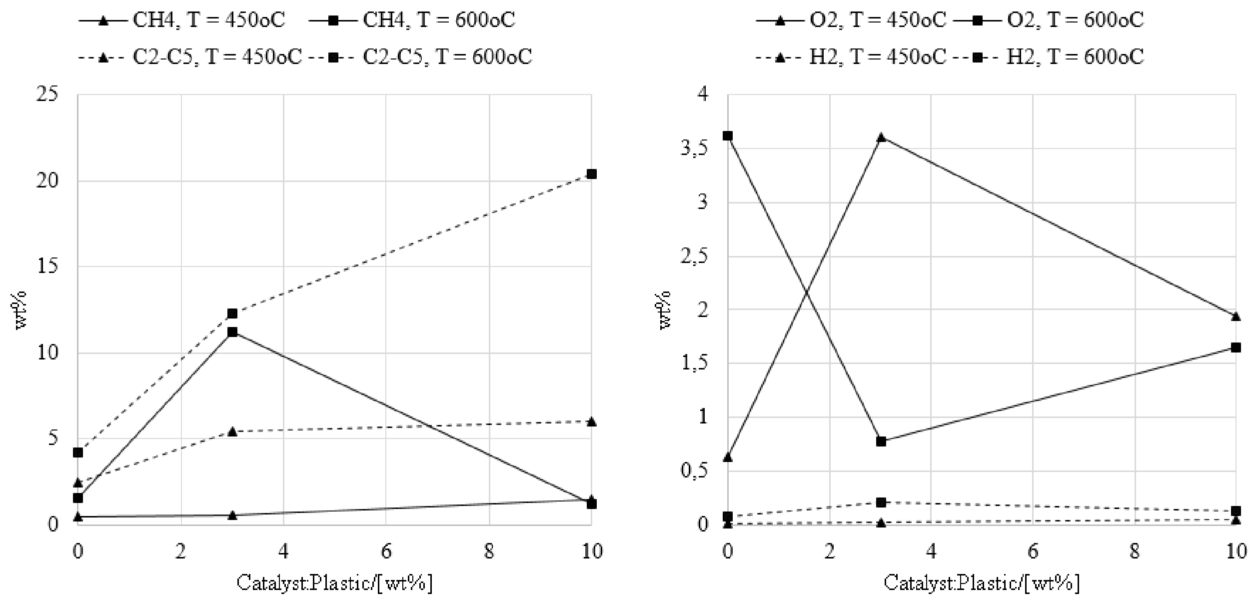

Figure 9: CH_4 (left, solid line, ±1.50 wt%), C_2-(C5) hydrocarbons (left, dashed line, ±2.73 wt%), O_2 (right, solid line, ±1.30 wt%) and H_2 (right, dashed line, ±0.09 wt%) yield (in wt%) at 450 ^oC (triangles) and at 600 ^oC (squares) at 20s residence time and catalyst:plastic mass ratio of 0-10 wt%

However, when the oxygen is available at the surface of a catalyst as in this case and not in the gas phase the formation of CO_2 is suppressed and the selectivity of C_2-C_5 hydrocarbons increases [58] explaining the reduction of CH_4 and CO_2 and increase in C_2-C_5 yield at high temperature (600 ^oC) shown in Figure 9.

However, it was found that part of the SO_4 group decomposed into SOx, specially at temperatures above 525 ^oC. TGA analysis of SZ performed by Srinivasan et al. [59] showed two weight loss regions for SZ in helium; an initial 10 wt% weight loss between 100-500 ^oC and a second 6 wt% weight loss between 500-700 ^oC. Therefore for temperatures above 525 ^oC, higher catalyst loads were needed to promote secondary reactions to form light hydrocarbons rather than CO_2 since as the catalyst was decomposed the number of active sites was decreased. Further discussion on SZ thermal decomposition and deactivation is discussed later on in section 3.4.

3.3. Effect of operating conditions on the wax composition

According to ^{1}H-NMR, PET wax was formed by aromatic compounds (peaks mostly appeared within 6.6-8.3ppm region). Shown in Figure 10 is the calculated proportion of aromatic and olefinic fractions presented in the wax obtained by ^{1}H-NMR analysis based on the method proposed by Myers et al. [60].

The olefin content corresponded to the functional groups that are attached to the benzene ring. This confirms the presence of vinyl ester groups in the wax product identified by the GC-MS analysis. The aromatic percentage corresponded to the hydrogen atoms that are attached to the aromatic ring implying that most of the wax product is formed by aromatic compounds as identified by GC-MS analysis. Increasing pyrolysis temperature caused a slight increase in the functional groups at the expense of aromatic content

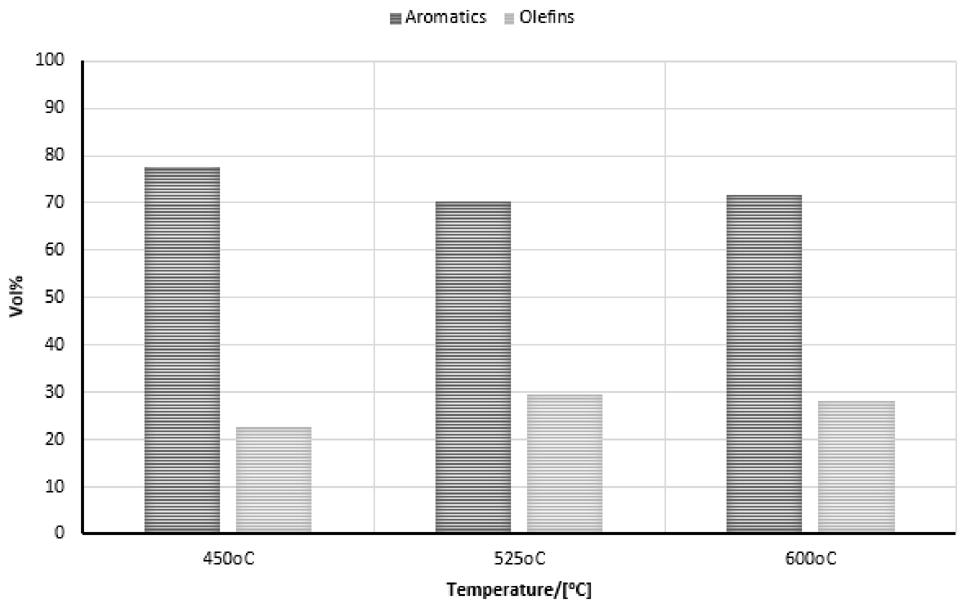

Figure 10: Proportion of aromatic and olefinic fraction in PET wax derived from pyrolysis at 450^{o}C, 525^{o}C and 600^{o}C at 20s volatiles residence time and 6.5wt% catalyst:plastic mass ratio

due to further decomposition of the primary compounds as described in Figure 11. However, ^{1}H-NMR results did not show a major difference because they only provide a general composition i.e. aromatic and olefinic, but did not provide information on the individual compounds or functional groups within those two wide fractions. Therefore, the wax was also qualitatively analysed by FT-IR and GC-MS and quantified via GC-FID as shown in sections 3.3.1 and 3.3.2.

3.3.1. Functional groups in PET wax product

The FT-IR analysis of the wax obtained at 450 ^{o}C, 525 ^{o}C and 600 ^{o}C, without catalyst at 20 s residence time are shown in Figure 12. As observed, temperature did not have an effect on the functional groups distribution in the wax fraction except for the presence of two small peaks between 3013-2815 cm^{-1} at 450 ^{o}C which were not present at 525 ^{o}C and 600 ^{o}C. These two peaks corresponding to the C-H stretch in the methylene group (R=CH_2) suggested that as temperature increased the vinyl ester bond decomposes into other compounds. The presence of the most predominant peak at 1730-1630 cm^{-1} related to the C=O stretch and the peak between 1330-1200 cm^{-1} designated to the C-O stretch implies the existence of carboxylic acids (the second peak typically found between 1380-1210 cm^{-1}) or esters (the second peak usually between 1300-1100 cm^{-1}) [61, 62].

The findings from the FT-IR analysis agreed well with those obtained from ^{1}H-NMR and GC-MS with a significant proportion of aromatic compounds (70-80vol%) and olefins (20-30vol%). Peaks around 1000cm^{-1} and 900cm^{-1} corresponded to the C-C and C-H stretch in aromatic rings respectively. These findings confirmed that PET wax was formed mainly by aromatic compounds and therefore it presented a low H/C ratio as expected. The FT-IR spectrum from PET pyrolysis wax showed in Figure 12 also agrees with

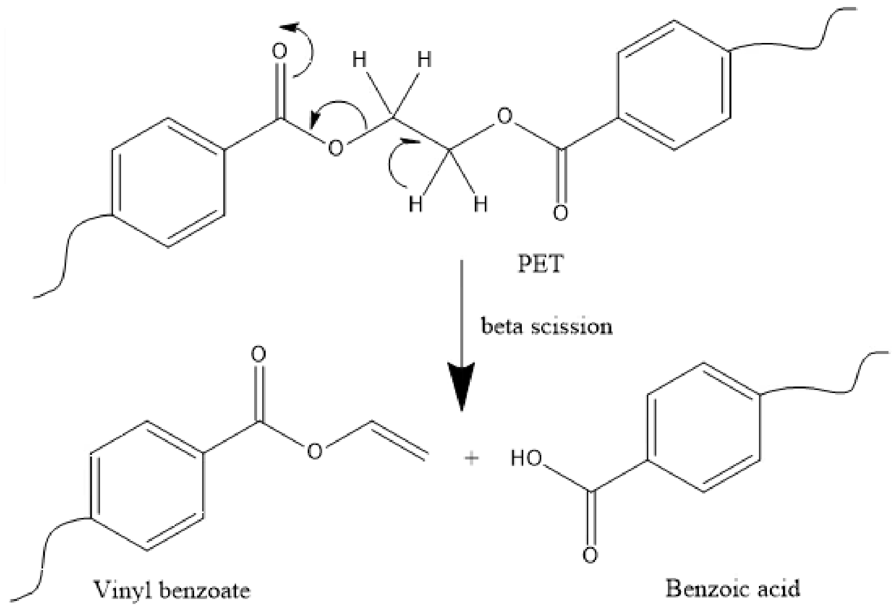

Figure 11: Beta scission mechanism of PET thermal degradation adapted from [24]

previous spectra reported in literature [51].

3.3.2. Wax composition

Based on ^{1}H-NMR and FT-IR results, it can be concluded that the majority of the wax was aromatic compounds. The GC-MS results confirmed that 90-95% of pyrolysis wax comprised of: benzaldehyde, acetophenone, methoxybenzyl alcohol, benzoic ether, benzoic acid and 2-acetylbenzoic acid which agreed well with previous studies [21, 24, 51, 63]. The yields of individual components and the effect of temperature and catalyst:plastic mass ratio on the product distribution are summarised in Figure 3. The GC-FID results showed that the product distribution of PET pyrolysis wax was as follows: 19.02-31.64 wt% of benzoic acid; 1.18-5.88 wt% of acetylbenzoic acid; 0.72-3.22 wt% of benzoic ether; 1.05-2.21 wt% of acetophenone; 0.40-1.22 wt% of styrene; 0.06-0.92 wt% of methoxybenzyl alcohol and the difference by other aromatic compounds (1.82-6.47 wt%) which agrees with composition already suggested in literature [7, 64].

As shown in Figure 11, PET decomposition is initiated (>395 ^{o}C) by beta scission at the carboxylic group where the ester link is broken to form benzoic acid and vinyl benzoate. As temperature keeps increasing the amount of vinyl benzoate formed further decomposes into other aromatic compounds in the wax fraction and lighter compounds in the gas phase. Theoretically, vinyl benzoate undergoes a McLafferty rearrangement yielding acetaldehyde and ethylene [24]. However, acetaldehyde was not found for any of the tested conditions and it is not reported as a product from neither thermal nor catalytic PET pyrolysis in literature [7, 21, 51, 63, 64]. The addition of SZ provides both Brønsted and Lewis acid sites [40]. Lewis acidic sites correspond to the zirconia (Zr) atoms while the Brønsted acidic sites are protons on the surface hydroxyl groups of sulfated zirconia oxide as shown in Figure 13. Those active sites promote the formation of carbocations

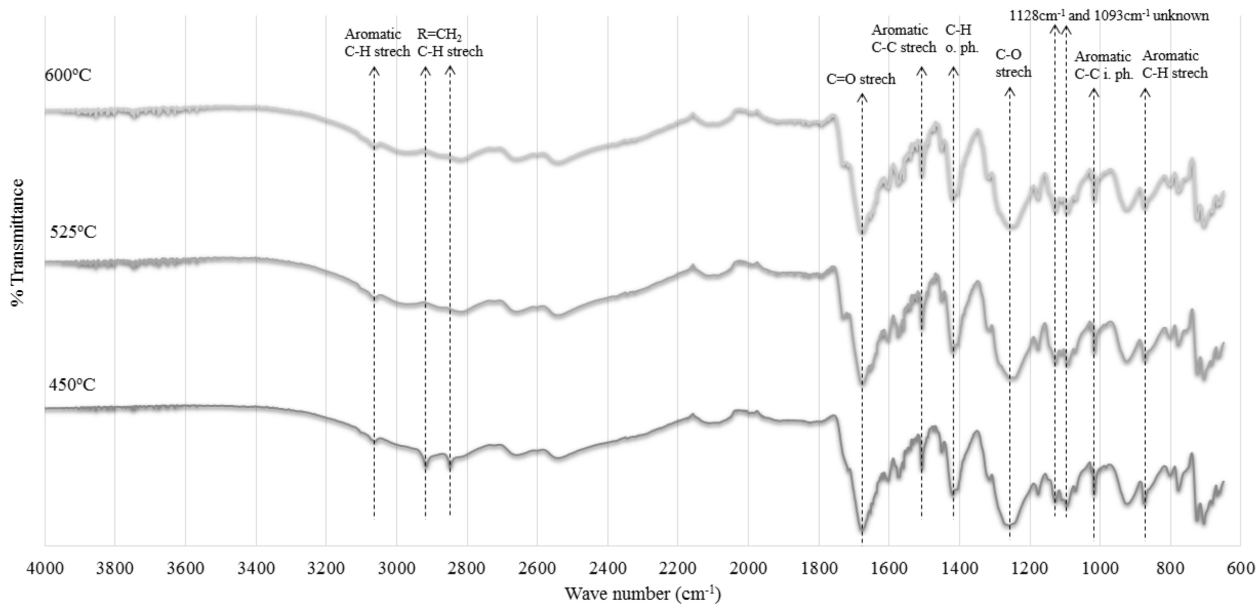

Figure 12: FT-IR spectrums of PET wax obtained at 450^{o}C (bottom), 525^{o}C (middle) and 600^{o}C (top) without catalyst at 20s residence time.

on the surface of the species formed by thermal decomposition via proton donation (Brønsted) or electron acceptance (Lewis) creating active species that further crack into smaller molecules.

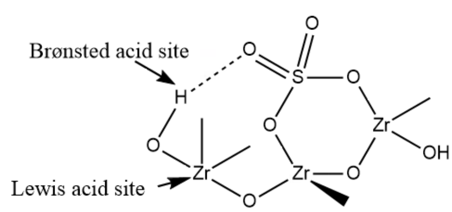

Figure 13: Scheme of the Brønsted and Lewis acid sites on SZ. Adapted from [46]

Temperature and catalyst to plastic mass ratio were the main parameters affecting the formation of benzoic acid (Figure 3). When the temperature increased from 450 ^{o}C to 600 ^{o}C the amount of benzoic acid decreased by 26 % (26.9 wt% to 20.0 wt% ± 1.7 wt%) at 3 wt% catalyst:plastic mass ratio but remained the same (27.4 wt% to 28.0 wt% ± 1.7wt%) at 10 wt% catalyst:plastic mass ratio. At low temperature (450^{o}C) the amount of benzoic acid remain unchangeable (26.9 - 27.5 wt% ± 1.7 wt%) with increasing catalyst:plastic mass ratio from 3 wt% to 10 wt% whereas it was 40 % increase at high temperature i.e. 600 ^{o}C (20.0 wt% to 28.0 wt% ± 1.7 wt%).

3.4. Sulfated zirconia thermal decomposition and deactivation

During this study it was found that the SZ catalyst was deactivated due to coke deposition and was partially decomposed at temperatures above 525 ^{o}C i.e. the weight of SZ after pyrolysis recovered from

Table 3: Variation of PET catalytic pyrolysis wax with temperature (450-600 ^{o}C) and catalyst:plastic (C/P) mass ratio (0-10 wt%) at 20s volatile residence time. Yield of compound $i = Masscompoundi/InitialPETmass$ where the mass of each compound was extracted from GC-FID via internal standard calibration. Legend: (a) Styrene (±0.44 wt%), (b) acetophenone (±0.61 wt%), (c) methoxybenzyl alcohol (±1.13 wt%), (d) benzoic ether (±1.54 wt%), (e) benzoic acid (±2.67 wt%), (f) acetylbenzoic acid (±0.07 wt%) and (g) other unknown aromatics (±4.84 wt%) calculated by difference, T = Temperature/[^{o}C], VRT = Volatiles residence time/[s], C:P = Catalyst:Platic/[wt%]

		Product/[wt%]						
T	C:P	(a)	(b)	(c)	(d)	(e)	(f)	(g)
450	0	0.59	1.84	0.90	1.36	27.13	1.66	1.82
	3	1.00	2.21	0.88	3.15	27.53	2.93	3.71
	10	0.40	1.05	0.04	0.99	25.24	1.18	2.69
525	0	0.79	1.21	0.06	2.73	23.91	1.95	3.62
600	0	1.22	2.10	0.08	3.22	31.64	5.88	5.21
	3	0.48	1.60	0.92	1.75	19.02	2.81	4.15
	10	0.45	1.10	0.45	0.72	25.91	2.86	6.47

the catalyst bed was lower than the initial load. The latter explained the low benzoic acid yield at 600 ^{o}C and catalyst:plastic mass ratio of 1/30 (i.e. 3 wt%) compared to the equivalent at 450 ^{o}C as shown in Table 3. To understand the behaviour of SZ under high temperature, SZ catalyst thermal transitions were studied in a TA Instruments Q20 differential scanning calorimeter at 5 ^{o}C/min from 30 - 550 ^{o}C. Four exothermic peaks were found at: 82.58, 177.43, 455.53 and 525.17 ^{o}C. The first two peaks (between 80-180 ^{o}C) were caused by the loss of hydrated water molecules from the zirconium sulphate hydrate ($ZrSO_{42}\cdot xH_2O$) according to the following reaction: $Zr(SO_4)_2 \cdot x\mathrm{H_2O} \rightarrow Zr(SO_4)_2 \cdot y\mathrm{H_2O}$ where y<x. The third and fourth endothermic peaks (between 455 and 525 ^{o}C) were either caused by the crystallisation of tetragonal ZrO_2 according to: $Zr(SO_4)_2 \rightarrow \mathrm{ZrO_2} + gases$ or by the decomposition of the sulphate into SO_x gases and O_2. This decomposition was previously reported to occur at temperatures above 700 ^{o}C [65]. Despite Wang et al. [66] suggestion that under N_2 the sulphur content of SZ decreases at temperatures above 500 ^{o}C, possibly explaining the peak obtained at 525.17 °C, no sulphur compounds were found were detected during experiments at any temperature in neither the gas not the wax fraction. Therefore, the SZ weight loss observed after pyrolysis at high temperature is caused by the loss of hydrated water along with the crystallisation of tetragonal ZrO_2.

SZ deactivation was reported due to either the reduction of the surface sulphate groups from S^{+6} to lower oxidation states at temperatures above 400 ^{o}C, decreasing both the acidity and activity of the catalyst or due to pore clogging via formation of coke during reaction [67]. SZ deactivation was further studied for another decomposition process of plastic waste [68]. SZ and zeolite HY were both re-used up to four consecutive plastic waste pyrolysis cycles before they showed similar yields than thermal pyrolysis i.e. deactivation of the catalyst caused by coke deposition in the catalyst pores. Deactivated zeolite HY was partially recovered in a parallel work by heating up to 600 ^{o}C in a CO_2 atmosphere. Up to 77 % of the carbon was removed and the catalyst recovered catalyst performed in a similar way as to spent catalyst after two cycles. Therefore, SZ deactivation due to coke formation could be also recovered by the method mentioned above.

Despite the SZ partial decomposition, SZ has advantages as a catalyst in terms of cost and environmental impact compared to other commercial catalyst such as zeolites, even though it may not be suitable for PET pyrolysis at high temperatures (600 ^oC). When combining catalyst and thermal pyrolysis at 450 ^oC, the yield of benzoic acid was up to 27.0 $\pm$ 1.7 wt% and partial decomposition of the catalyst due to temperature was not observed. This yield was comparable with the one obtained at higher temperatures (20.0 $\pm$ 1.7 wt% at 525 ^oC and 10 wt% catalyst and 28.0 $\pm$ 1.7 wt% at 600 ^oC and 10 wt% catalyst).

Unlike PET glycolysis where the catalyst is commonly in a liquid form that needs to be separated from the products and cannot be reused, SZ is a solid catalyst that is placed on a separate bed and therefore not mixed with pyrolysis products. SZ deactivation was caused by coke deposition and therefore is reversible through regeneration by combustion at 450 ^oC [69, 70] or treatment with hydrogen [71], allowing the reutilization of the catalyst. From previous studies [68], SZ could also be used for several pyrolysis cycles before complete deactivation which then be regenerated for further used without losing its activity. Therefore, the use of this catalyst showed some enhancement over conventional PET pyrolysis and could be considered as an alternative catalyst for low temperature PET pyrolysis.

Assuming an average 24 wt% benzoic acid yield recovered from PET waste, potentially about 408 ktons of benzoic acid could be recovered if all PET waste generated were managed by PET pyrolysis. This could suggest a recovery value of almost $1.8 million per year assuming steady PET waste generation as in the UK in 2014 [1]. In addition, PET waste pyrolysis could avoid the disposal of over 600ktons of PET waste in landfills assuming an average plastic waste landfill disposal rate in the UK of 38 wt% (plastic waste landfill disposal rate in the UK in 2014 [1]).

4. Conclusions

PET is one of the most common plastic waste generated everyday all over the world and is mainly used in food packaging applications which suggests a very short life and consequent rapid generation of PET waste. Currently, chemical recycling through glycolysis and landfill are the main approaches for PET waste management in the EU and USA. Pyrolysis is a promising alternative to recover valuable chemicals without extra costs associated with cleaning and segregation of plastic waste like in glycolysis or mechanical recycling. The results showed that both catalyst:plastic mass ratio and temperature play an important role in the production of benzoic acid, a precursor widely used in the food and beverage industry. High temperature (600^oC) and no catalyst increased by 16% the benzoic acid recovery in the wax product compared to the other conditions tested. However, operation at those conditions is energy intensive due to the energy consumption to achieve high temperature since pyrolysis of PET is an endothermic process. The addition of the catalyst increased the amount of another valuable product i.e. light hydrocarbons (C_1-C_4) from 4wt% without catalyst to 20wt% at 10wt% catalyst:plastic ratio. SZ deactivated due to coke deposition on the catalyst surface as well as partially decomposed at high pyrolysis temperatures i.e. >525^{o}C. This phenomena was not observed when pyrolysis was performed at low temperatures. Based on the costs of catalyst and energy (about $1.4/g (anhydrous) SZ versus $0.10/kW-h on average in 2015 in the IEA [72]), results from this study suggest that PET catalytic pyrolysis in the presence of SZ should be carried out at temperatures below 525^{o}C and catalyst loads below 10wt.% to obtain high yields of benzoic acid and high value of gas products i.e. high proportion of hydrocarbons.

Acknowledgments

PET waste were kindly provided by O'Brien Recycling Solutions (Wallsend, Newcastle upon Tyne, UK). CHN analysis and X-ray diffraction spectra were obtained at Advanced Chemical and Materials Analysis (ACMA) at Newcastle University and we would like to thank Richard Baron and Maggie White who respectively performed those analysis. ^{1}HNMR analysis was conducted at the School of Chemistry, Newcastle University, by Dr Corinne Willis who we thank for her collaboration.

References

[1] Plastic Europe, Plastic - the facts 2014-2015 (November 11/05/2016).
URL `http://www.plasticseurope.org/Document/plastics-the-facts-2014.aspx?Page=DOCUMENT&FolID=2`

[2] N. Themelis, C. Mussche, 2014 Energy and economic value of municipal solid waste (MSW), including non-recycled plastics (NRP), currently landfilled in the fifty, https://www.americanchemistry.com/Policy/Energy/Energy-Recovery/2014-Update-of-Potential-for-Energy-Recovery-from-Municipal-Solid-Waste-and-Non-Recycled-Plastics.pdf.

[3] (Trucost), J. Raynaud, Valuing Plastics: The Business Case for Measuring, Managing and Disclosing Plastic Use in the Consumer Goods Industry, Technical report, UNEP (2014).
URL `www.unep.org/pdf/ValuingPlastic/`

[4] Eurostat, Municipal waste (May 30/05/2016).
URL `http://ec.europa.eu/eurostat/cache/metadata/en/env_wasmun_esms.htm`

[5] Eurostat, Municipal waste landfilled, incinerated, recycled and composted in the eu-27, 1995 to 2014 (May 30/05/2016).
URL `http://ec.europa.eu/eurostat/statistics-explained/index.php/File:Municipal_waste_landfilled,_incinerated,_recycled_and_composted_in_the_EU-27,_1995_to_2014.png#file`

[6] L. Bartolome, B. Cho, H. Do, M. Imran, W. Al-Masry, Recent Developments in the Chemical Recycling of PET, INTECH Open Access Publisher, 2012.

[7] S. Du, J. Valla, R. Parnas, G. Bollas, Conversion of polyethylene terephthalate based waste carpet to benzene-rich oils through thermal, catalytic, and catalytic steam pyrolysis, ACS Sustainable Chemistry & Engineering 4 (5) (2016) 2852–2860.

[8] WRAP, Realising the value of recovered plastic - Market Situation Report, Tech. rep., WRAP (2010).

[9] The Telegraph, Plastic waste 'already building up in UK' following China's ban (05/02/2018). URL http://www.telegraph.co.uk/news/2018/01/02/plastic-waste-already-building-uk-following-chinas-ban/

[10] European Commission, Plastic Waste: Ecological and Human Health Impacts, Tech. rep., Science for Environment Policy: DG Environment News Alert Service, accessed 11/05/2017 (2011). URL http://ec.europa.eu/environment/integration/research/newsalert/pdf/IR1_en.pdf

[11] J. Aguado, D. Serrano, G. San Miguel, European trends in the feedstock recycling of plastic wastes, Global Nest J 9 (1) (2007) 12–19.

[12] J. Hopewell, R. Dvorak, E. Kosior, Plastics recycling: challenges and opportunities, Philosophical Transactions of the Royal Society B: Biological Sciences 364 (1526) (2009) 2115–2126.

[13] B. Johnke, R. Hoppaus, E. Lee, B. Irving, T. Martinsen, K. Mareckova, Good Practice Guidance and Uncertainty Management in National Greenhouse Gas Inventories - Emissions from waste incineration, Tech. rep., Intergovernmental Panel on Climate Change - IPCC (2001). URL http://www.ipcc-nggip.iges.or.jp/public/gp/bgp/5_3_Waste_Incineration.pdf

[14] European Commission (EC), , Integrated Pollution Prevention and Control (IPPC) - Reference Document on the Best Available Techniques for Waste Incineration, Tech. rep., European Commission (2006).

[15] A. Buekens, H. Huang, Comparative evaluation of techniques for controlling the formation and emission of chlorinated dioxins/furans in municipal waste incineration, Journal of Hazardous Materials 62 (1) (1998) 1–33.

[16] D. Carta, G. Cao, C. D,Angeli, Chemical recycling of poly(ethylene terephthalate)(PET) by hydrolysis and glycolysis, Environmental Science and Pollution Research 10 (6) (2003) 390–394.

[17] Q. Yue, C. Wang, L. Zhang, Y. Ni, Y. Jin, Glycolysis of poly (ethylene terephthalate)(PET) using basic ionic liquids as catalysts, Polymer degradation and stability 96 (4) (2011) 399–403.

[18] G. Karayannidis, D. Achilias, Chemical recycling of poly(ethylene terephthalate), Macromolecular Materials and Engineering 292 (2) (2007) 128–146.

[19] M. Khoonkari, A. Haghighi, Y. Sefidbakht, K. Shekoohi, A. Ghaderian, Chemical recycling of PET wastes with different catalysts, International Journal of Polymer Science 2015.

[20] D. Paszun, T. Spychaj, Chemical recycling of poly(ethylene terephthalate), Industrial & Engineering Chemistry Research 36 (4) (1997) 1373–1383.

[21] M. Dzięcioł, J. Trzeszczyński, Volatile products of poly (ethylene terephthalate) thermal degradation in nitrogen atmosphere, Journal of Applied Polymer Science 77 (9) (2000) 1894–1901.

[22] S. Kumagai, I. Hasegawa, G. Grause, T. Kameda, T. Yoshioka, Thermal decomposition of individual and mixed plastics in the presence of cao or ca (oh) 2, Journal of Analytical and Applied Pyrolysis 113 (2015) 584–590.

[23] D. Nikles, M. Farahat, New motivation for the depolymerization products derived from poly(ethylene terephthalate)(PET) waste: a review, Macromolecular Materials and Engineering 290 (1) (2005) 13–30.

[24] S. Venkatachalam, A. Kelkar, J. Labde, K. Rao, P. Gharal, S. Nayak, Degradation and Recyclability of Poly (Ethylene Terephthalate), INTECH Open Access Publisher, 2012.

[25] Global Market Insights, Benzoic Acid Market Size, Industry Analysis Report, Regional Outlook (U.S., Germany, UK, Italy, Russia, China, India, Japan, South Korea, Brazil, Mexico, Saudi Arabia, UAE, South Africa), Application Development, Price Trend, Competitive Market Share and Forecast, 2016 - 2023 (January 25/01/2017).
URL https://www.gminsights.com/industry-analysis/benzoic-acid-market

[26] C. Loong, Simulation: Optimize the production of benzoic acid by using benzene and acetic anhydride, Universiti Tunku Abdul Rahman, 2011.

[27] A. Garforth, Y. Lin, P. Sharratt, J. Dwyer, Production of hydrocarbons by catalytic degradation of high density polyethylene in a laboratory fluidised-bed reactor, Applied Catalysis A: General 169 (2) (1998) 331–342.

[28] G. Luo, T. Suto, S. Yasu, K. Kato, Catalytic degradation of high density polyethylene and polypropylene into liquid fuel in a powder-particle fluidized bed, Polymer Degradation and Stability 70 (1) (2000) 97–102.

[29] Y. Xue, S. Zhou, R. Brown, A. Kelkar, X. Bai, Fast pyrolysis of biomass and waste plastic in a fluidized bed reactor, Fuel 156 (2015) 40–46.

[30] I. Martın-Gullon, M. Esperanza, R. Font, Kinetic model for the pyrolysis and combustion of poly-(ethylene terephthalate)(PET), Journal of Analytical and Applied Pyrolysis 58 (2001) 635–650.

[31] R. Lin, D. Negelein, R. White, Effects of catalyst acidity and structure on polymer cracking mechanisms, online (1995).
URL https://web.anl.gov/PCS/acsfuel/preprint%20archive/Files/42_4_LAS%20VEGAS_09-97_0982.pdf

[32] S. Sharuddin, F. Abnisa, W. Daud, M. Aroua, A review on pyrolysis of plastic wastes, Energy Conversion and Management 115 (2016) 308–326.

[33] J. Wu, T. Chen, X. Luo, D. Han, Z. Wang, J. Wu, TG/FTIR analysis on co-pyrolysis behavior of PE, PVC and PS, Waste management 34 (3) (2014) 676–682.

[34] O. Cepeliogullar, A. Putun, Utilization of two different types of plastic wastes from daily and industrial life, Journal of Selcuk University Natural and Applied Science (2013) 694–706.

[35] J. Onwudili, N. Insura, P. Williams, Composition of products from the pyrolysis of polyethylene and polystyrene in a closed batch reactor: Effects of temperature and residence time, Journal of Analytical and Applied Pyrolysis 86 (2) (2009) 293–303.

[36] W. Kaminsky, J. Kim, Pyrolysis of mixed plastics into aromatics, Journal of Analytical and Applied Pyrolysis 51 (1-2) (1999) 127–134.

[37] T. Bhaskar, M. Uddin, K. Murai, J. Kaneko, K. Hamano, T. Kusaba, A. Muto, Y. Sakata, Comparison of thermal degradation products from real municipal waste plastic and model mixed plastics, Journal of Analytical and Applied Pyrolysis 70 (2) (2003) 579–587.

[38] R. Lin, R. White, Acid-catalyzed cracking of polystyrene, Journal of applied polymer science 63 (10) (1997) 1287–1298.

[39] J. Chattopadhyay, T. Pathak, R. Srivastava, A. Singh, Catalytic co-pyrolysis of paper biomass and plastic mixtures (HDPE (high density polyethylene), PP (polypropylene) and PET (polyethylene terephthalate)) and product analysis, Energy 103 (2016) 513–521.

[40] R. Srinivasan, R. Keogh, B. Davis, Sulfated zirconia catalysts: Are Brønsted acid sites the source of the activity?, Catalysis letters 36 (1-2) (1996) 51–57.

[41] X. Li, K. Nagaoka, L. Simon, J. Lercher, S. Wrabetz, F. Jentoft, C. Breitkopf, S. Matysik, H. Papp, Interaction between sulfated zirconia and alkanes: prerequisites for active sites-formation and stability of reaction intermediates, Journal of Catalysis 230 (1) (2005) 214–225.

[42] Z. Helwani, M. Othman, N. Aziz, W. Fernando, J. Kim, Technologies for production of biodiesel focusing on green catalytic techniques: a review, Fuel Processing Technology 90 (12) (2009) 1502–1514.

[43] E. Eterigho, J. Lee, A. Harvey, Triglyceride cracking for biofuel production using a directly synthesised sulphated zirconia catalyst, Bioresource technology 102 (10) (2011) 6313–6316.

[44] M. Van der Stelt, H. Gerhauser, J. Kiel, K. Ptasinski, Biomass upgrading by torrefaction for the production of biofuels: A review, Biomass and bioenergy 35 (9) (2011) 3748–3762.

[45] E. Eterigho, Development and Application of Heterogeneous Catalysts for Direct Cracking of Triglycerides for Biodiesel Production, Newcastle University, 2012.

[46] L. Wang, F. Xiao, Nanoporous catalysts for biomass conversion, Green Chemistry 17 (1) (2015) 24–39.

[47] N. Tangchupong, W. Khaodee, B. Jongsomjit, N. Laosiripojana, P. Praserthdam, S. Assabumrungrat, Effect of calcination temperature on characteristics of sulfated zirconia and its application as catalyst for isosynthesis, Fuel Processing Technology 91 (1) (2010) 121–126.

[48] L. Hamouda, A. Ghorbel, F. Figueras, Study of acidic and catalytic properties of sulfated zirconia prepared by sol-gel process: Influence of preparation conditions, Studies in Surface Science and Catalysis 130 (2000) 971–976.

[49] W. Stichert, F. Schüth, Synthesis of catalytically active high surface area monoclinic sulfated zirconia, Journal of Catalysis 174 (2) (1998) 242–245.

[50] L. Diaz Silvarrey, A. Phan, Kinetic study of municipal plastic waste, International Journal of Hydrogen Energy 41 (37) (2016) 16352–16364.

[51] I. Çit, A. Sınağ, T. Yumak, S. Uçar, Z. Mısırlıoğlu, M. Canel, Comparative pyrolysis of polyolefins (PP and LDPE) and PET, Polymer bulletin 64 (8) (2010) 817–834.

[52] F. Mastral, E. Esperanza, C. Berrueco, M. Juste, J. Ceamanos, Fluidized bed thermal degradation products of HDPE in an inert atmosphere and in air–nitrogen mixtures, Journal of Analytical and Applied Pyrolysis 70 (1) (2003) 1–17.

[53] C. Ludlow-Palafox, H. Chase, Microwave-induced pyrolysis of plastic wastes, Industrial & engineering chemistry research 40 (22) (2001) 4749–4756.

[54] T. Reed, The Boudouard Equilibrium - Gasifiers (12/01/2016).
URL http://gasifiers.bioenergylists.org/files/boudouard_reaction.xls

[55] P. Lahijani, Z. Zainal, M. Mohammadi, A. Mohamed, Conversion of the greenhouse gas CO_2 to the fuel gas co via the boudouard reaction: A review, Renewable and Sustainable Energy Reviews 41 (2015) 615–632.

[56] M. Kogler, E. KoÌĹck, B. KloÌĹtzer, T. Schachinger, W. Wallisch, R. Henn, C. Huck, C. Hejny, S. Penner, High-temperature carbon deposition on oxide surfaces by CO disproportionation, The Journal of Physical Chemistry C 120 (3) (2016) 1795–1807.

[57] B. Eliasson, C. Liu, U. Kogelschatz, Direct conversion of methane and carbon dioxide to higher hydrocarbons using catalytic dielectric-barrier discharges with zeolites, Industrial & Engineering Chemistry Research 39 (5) (2000) 1221–1227.

[58] T. Nishiyama, K. Aika, Mechanism of the oxidative coupling of methane using C_{02} as an oxidant over PbO–MgO, Journal of Catalysis 122 (2) (1990) 346–351.

[59] R. Srinivasan, R. Keogh, D. Milburn, B. Davis, Sulfated zirconia catalysts: Characterization by tga/dta mass spectrometry, Journal of Catalysis 153 (1) (1995) 123–130.

[60] M. Myers Jr, J. Stollsteimer, A. Wims, Determination of hydrocarbon-type distribution and hydrogen/carbon ratio of gasolines by nuclear magnetic resonance spectrometry, Analytical Chemistry 47 (12) (1975) 2010–2015.

[61] P. Larkin, Chapter 7 - General Outline and Strategies for IR and Raman Spectral Interpretation, in: Infrared and Raman Spectroscopy, Elsevier, Oxford, 2011, pp. 117–133.

[62] T. Masuda, Y. Miwa, A. Tamagawa, S. Mukai, K. Hashimoto, Y. Ikeda, Degradation of waste poly(ethylene terephthalate) in a steam atmosphere to recover terephthalic acid and to minimize carbonaceous residue, Polymer degradation and stability 58 (3) (1997) 315–320.

[63] T. Yoshioka, G. Grause, C. Eger, W. Kaminsky, A. Okuwaki, Pyrolysis of poly(ethylene terephthalate) in a fluidised bed plant, Polymer Degradation and Stability 86 (3) (2004) 499 – 504.

[64] E. Dziwiński, J. Iłowska, J. Gniady, Py-GC/MS analyses of poly(ethylene terephthalate) film without and with the presence of tetramethylammonium acetate reagent. Comparative study, Polymer Testing 65 (2018) 111–115.

[65] J. Sohn, D. Lee, Characterization of zirconium sulfate supported on TiO_2 and activity for acid catalysis, Korean Journal of Chemical Engineering 20 (6) (2003) 1030–1036.

[66] P. Wang, J. Zhang, G. Wang, C. Li, C. Yang, Nature of active sites and deactivation mechanism for n-butane isomerization over alumina-promoted sulfated zirconia, Journal of Catalysis 338 (2016) 124–134.

[67] F. Ng, N. Horvát, Sulfur removal from ZrO_2/so_4^{2-} during n-butane isomerization, Applied Catalysis A: General 123 (2) (1995) L197–L203.

[68] L. Diaz-Silvarrey, K. Zhang, A. Phan, Monomer recovery through advanced pyrolysis of waste high density polyethylene (HDPE), Green Chemistry 20 (2018) 1813–1823.

[69] L. Binghui, Deactivation and regeneration of sulfated zirconia, Ph.D. thesis, Tulane University, New Orleans, Luisiana, USA (1998).
URL https://digitallibrary.tulane.edu/islandora/object/tulane%3A24803

[70] C. Li, P. Stair, Ultraviolet raman spectroscopy characterization of sulfated zirconia catalysts: fresh, deactivated and regenerated, Catalysis letters 36 (3) (1996) 119–123.

[71] Y.-C. Yang, H.-S. Weng, Regeneration of coked al-promoted sulfated zirconia catalysts by high pressure hydrogen, Industrial & Engineering Chemistry Research 49 (4) (2010) 1982–1985.

[72] UK Department for Business, Energy & Industrial Strategy, Industrial electricity prices in the IEA (QEP 5.3.1) (January 25/01/2017).
URL https://www.gov.uk/government/statistical-data-sets/international-industrial-energy-prices

1) PET wastes are rising however its management is still not sustainable
2) In this study, sulphated zirconia was first time used for catalytic pyrolysis of PET
3) Up to 27-32wt% benzoic acid could be recovered through PET pyrolysis at 450-600^{o}C
4) Increasing the catalyst to 10wt% enhanced other valuable products i.e. C_1-C_3 hydrocarbons

Material recovery from waste polyethylene terephthalate (PET)

Laura S Diaz-Silvarrey*[a], Andrew McMahon[a], and Anh N. Phan*[a]

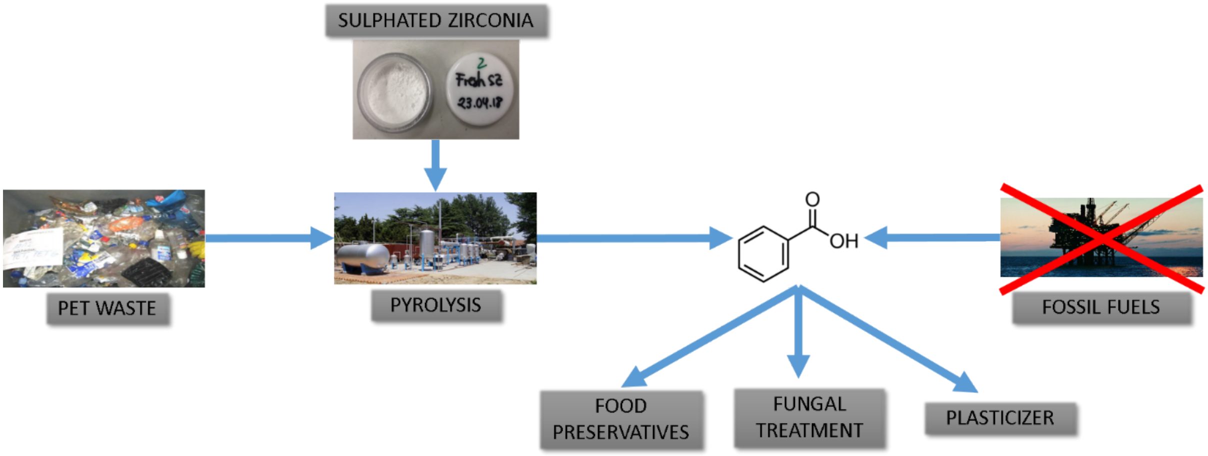

Pyrolysis of waste PET waste yielded up to 32 wt% of benzoic acid, widely used in the food industry

Material recovery from waste polyethylene terephthalate (PET)

Laura S Diaz-Silvarrey[a,*], Andrew McMahon[a], Anh N. Phan[a,**]

[a]*School of Engineering, Newcastle University, Newcastle upon Tyne*

Abstract

Polyethylene terephthalate (PET) is one of the main plastics used in food packaging products, which have a very short life and are rapidly transformed into waste, and accounts for 7wt% of the total plastic waste generated. Current PET waste management, mainly via mechanical recycling and glycolysis, have encountered a number of issues: negative impact on the environment, segregation of waste and product separation/purification. Therefore other versatile alternatives such as pyrolysis should be employed to recover value-added products from waste. Benzoic acid a precursor in the food and beverage industry, derived from PET via thermochemical conversion opposed to the current manufacturing process from fossil fuel-based feedstock is considered as a promising approach. In this study, the effect of operating conditions i.e. temperature, catalyst to plastic mass ratio and volatiles residence time and their interactions on product yields and properties were studied. Sulphated zirconia (SZ) was first time used for catalytic pyrolysis of PET due to its high acidity and environmentally friendly synthesis. Results showed that up to 27-32wt% benzoic acid could be recovered through PET pyrolysis at 450-600^{o}C at 20s residence time. By increasing the catalyst:plastic ratio to 10wt% only 26wt% of benzoic acid was recovered in the wax but it increased the amount of other valuable products i.e. light hydrocarbons (C_1-C_3) recovered in the gas.

Keywords: PET, plastic waste, pyrolysis, catalysis, sulphated zirconia

1. Introduction

Commodity plastics i.e. polyethylene terephthalate (PET), polystyrene (PS), polypropylene (PP), polyethylene (PE), polyvinyl-chloride (PVC), which are produced from petroleum-based products, have been widely used due to their versatility, durability, low weight and cost [1, 2]. This causes an increase in waste i.e. average 8.7% per year [3]. The current depletion of petroleum resources coupled with the growing concern of plastic waste and their damaging effect on the Environment and ecological systems, recovery of monomers from plastic waste is now more imperative than it has ever been.

In the European Union (EU), and in the UK, it is estimated that plastic waste contributes up to 10-13% of municipal solid waste (MSW) [4, 5], of which 7wt% (1.7 million tonnes) is PET [1]. PET is widely used in the textile and carpet industry, in the packaging of food products and in the production of bottles

*l.diaz-silvarrey@newcastle.ac.uk
**anh.phan@newcastle.ac.uk

[6, 7]. PET waste is usually managed by landfill disposal, chemical recycling (methanolysis, glycolysis, hydrolysis), energy recovery via incineration and mechanical recycling. Themelis and Mussche [2] reported that approximately 83 % of plastic waste was disposed in landfills while only 7 % was recycled and 10 % was converted into energy via waste-to-energy plants in the USA in 2014. Although recycling and recovery rates were higher in the EU in the same year (30 %), still around 31 % of plastic waste was disposed in landfills with the balance converted into energy via waste-to-energy plants [1]. However, due to lack of recycling capacity plastic waste used to be sent to China for treatment. For instance, from the almost 600 ktonnes of plastic waste recycled in 2009 in the UK about 75 % were shipped abroad [8]. Since the beginning of 2018, the Chinese Government implemented a ban to import plastic waste which has led to an accumulation of plastic waste in the UK [9] that require versatile and alternative management solutions.

Since plastic waste are non-biodegradable, their disposal in landfills causes a negative impact on ecology, human health and wildlife [10]. Incineration with energy recovery, a common approach that reduces considerably the volume of wastes and produces energy, also emits airborne pollutants such as CO_2, N_2O, NOx, NH_3, VOC, polychlorinated dibenzo-p-dioxins and dibenzofurans (PCDD/PCDF), HCl, HF and SO_2 [11–15]. Mechanical recycling of PET, done by melting and extrusion of PET wastes into fibres, produces products with limited applications e.g. drinking bottles and food-graded materials require the use of virgin PET manufactured from fossil fuels. Therefore, from a sustainable point of view, chemical recycling via glycolysis or pyrolysis is preferred as an alternative to recover of raw materials.

Glycolysis is the common PET chemical recycling method to recover bis(hydroxyethyl) terephthalate (BHTE) monomer. It is the depolymerisation of PET through the solvolytic chain cleavage into smaller molecules in the presence of ethylene glycol at temperature and pressure ranges of 190-240 ^{o}C and 0.1-0.6 MPa over a long reaction time (0.5-8 h) [16]. In addition, this process requires a basic catalyst to obtain a reasonable yield of BHTE i.e. 6-70 % [17] at milder conditions [18]. Most catalysts are liquids in the form of metal acetates [17, 19], titanium-phosphates [17], solid super acids [17], metal oxides [17], ionic liquids[19], hydrotalcites [19], or enzymes [19]. The main disadvantages of PET glycolysis are i) the requirement of clean and pure PET waste streams, therefore requiring high segregation costs [6, 11, 12]; ii) the use of liquid catalysts that required further separation from glycolysis products creating waste water that requires treatment; and iii) the catalysts cannot be reused after separation increasing operation costs. Further details can be found elsewhere [16, 18, 20] but will not be discussed here as they escape the scope of this work.

Pyrolysis is an advanced thermochemical conversion carried out in a non-oxidant atmosphere at temperatures between 400-700 ^{o}C with or without a catalyst. Pyrolysis of plastic waste yields three fractions: solid residue, formed by carbon residue and any inorganic element present in the original plastic product; gas, comprised of CH_4, H_2, CO_2, CO and C_2-C_5 hydrocarbons; and wax/liquid/oil which comprises of a mixture of aliphatic and aromatic hydrocarbons. Pyrolysis can be applied to recover valuable chemicals from PET without cleaning, waste segregation [1, 6], the use of liquid catalysts and extra reagents. Unlike glycolysis, where the monomer (BHTE) is recovered, pyrolysis of PET yields other aromatic and oxygenated compounds like acetaldehyde, vinyl benzoate or benzoic acid [21] due to the difference in the decomposition mechanism. Kumagai et al. [22] showed that CaO catalyst/steam increased the amount of benzoic acid recovered in PET pyrolysis at 600 ^{o}C from 1.83 wt% to 8.29 wt%. During glycolysis, PET ester link is substituted by the hyroxyl group from the reagent glycol forming oligomers or oligoester diols/polyols with hydroxyl terminal groups being the most common one BHTE [16, 23]. Pyrolysis of PET is also produced via the cleavage of the ester linkage. However, as there are no glycols present, the bond cleavage is produced by the effect of either temperature or both temperature and catalyst resulting in the formation of vinyl ester and carboxyl compounds. The vinyl ester could decompose further into other compounds such as acetaldehyde, acetophenone or light hydrocarbons (C_1-C_3) [24].

Benzoic acid, one of the products from PET pyrolysis, is mainly used in the food and beverage industry as an intermediate to produce benazoates and other related antifungal preservatives (such as E210, E211, E212 and E213) present in numerous common foods like soft drinks, coffee, salad dressings, etc. as well as one of the main feedstock for phenol manufacture [25]. Benzoic acid is also used as a precursor of other products such as plasticizers, fungal ointments for medical use, and as a calibrating substance for bomb calorimeters [25]. Its market size is expected to increase by almost 30% in the next few years (from 480 ktons in 2014 to 620 ktons in 2023) [25] and its price is around $4000/Mton [26]. Therefore, the recovery of this compound is as important as that of the monomer BHET because benzoic acid is currently manufactured by partial oxidation of toluene with oxygen in the presence of cobalt or manganese naphthenates.

Research on pyrolysis process for different types of plastic in the plastic waste stream has been carried out over the years [21, 27–37], but only focusing on the effects of individual parameters such as the pyrolysis temperature (300K to 1000K), the type of catalyst (HZSM-5, HUSY, HMOR, Z-N, Silica-Alumina, Zeolite-Beta and SZ [38]), ratio of plastic to catalyst (100:1 to 10:1), and heating rate (5, 10 and 20K/min). The effect of temperature was also studied focusing on reactions pathways and product yields and distribution from PET pyrolysis [30, 39]. However, none of these studies looked at the synergistic effect of the pyrolysis temperature and SZ catalyst. In this study, the interactions of temperature and plastic:catalyst mass ratio on the product distribution of PET waste pyrolysis to recover valuable chemicals, i.e. benzoic acid. SZ was chosen because (i) it is a super acid catalyst [40], i.e. it activates light alkanes at room temperature [41], that is found to be effective for cracking of long chain hydrocarbons (triglycerides/vegetable oil [42, 43] and polystyrene [38]) and (ii) an environmentally friendly alternative compared to catalysts mentioned previously. However, limited research has also been carried out using SZ catalyst for pyrolysis of plastic waste, particularly for PET and examining the viability of using SZ in comparison to other common catalysts applied in the pyrolysis process of PET [31].

2. Experimental methodology

2.1. Materials

PET samples were collected from O'Brien's Waste Recycling Solutions (Wallsend, Newcastle upon Tyne, UK). They were thoroughly washed with soap and water to eliminate any effects caused by unknown contaminants, and then cut into 1.5x1.5cm size. PET waste characterisation is shown in Table 1. PET waste had a H/C ratio similar to that of lignite and lower than that of biomass [44] implying a very low hydrogen content due to the existence the aromatic rings, ester and carboxylic group as shown in Figure 1. The high calorific value of PET was similar to that of bituminous (17-23MJ/kg) or lignite coal (15-27 MJ/kg).

Table 1: PET waste characterisation

	PET waste
High calorific value / [MJ/kg]	22.860±0.005
Volatile matter / [wt%]	87.62±0.26
Ash content / [wt%]	2.39±0.64
Empirical formula	$C_5H_5O_2$

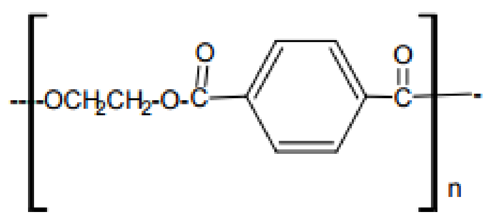

Figure 1: Structure of PET

2.2. Catalyst preparation and characterisation

SZ catalyst was synthesised by directly mixing zirconium (IV) oxychloride octahydrate (Sigma Aldrich) and ammonium sulphate (Sigma Aldrich) at 1:6 molar ratio followed by 18h ageing at constant temperature inside a VECSTAR VC1 horizontal furnace kept at 25^{o}C. The mixture was then calcined at 500^{o}C for 6h in the same furnace following the method described by Eterigho et al. [43]. The solvent free synthesis of SZ was proven to improve catalyst characteristics [45] due to a stronger interaction between SO_4^{2-} and ZrO_2 that reduces catalyst deactivation [46]. The morphology of the prepared catalyst was conducted using a Philips CM100 Transmission Electron Microscopy (TEM) with Compustage and high resolution digital image capture particle size distribution. Particle size distribution of the prepared catalyst was determined using Image J based on the TEM image shown in Figure 2. Results showed that around 60% of the particles were in the 1-2.9nm range while the rest were distributed from 2.9-4.8nm (15%), 4.8-6.7nm (10%) and 6.7-18.1nm (15%).

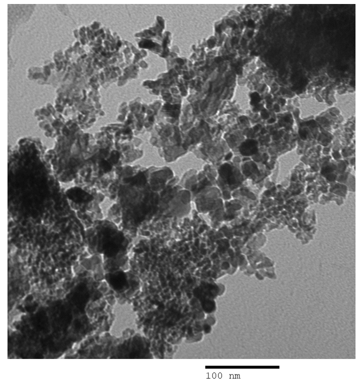

Figure 2: TEM image of SZ catalyst (180000x, HV = 100.0kV, scale = 100nm)

X-ray diffractograms (XRD) were obtained in a Panalytical X'Pert Pro Multopurpose Diffractometer (MPD) fitted with a X'Celerator and a secondary monochromator (Cu-Kα radiation, wavelength (λ) = 1.54$\mathring{A}$ generated at 40kV and 40mA) over a 2θ range of 2^o to 70^o from 2^{o}C - 100^{o}C. As shown in Figure 3, the sample was mainly amorphous with relatively low tetragonal and monoclinic phase crystalline fractions. The results were similar to those reported by Eterigho et al. [43] although the crystalline fraction of the SZ in this study was slightly higher.

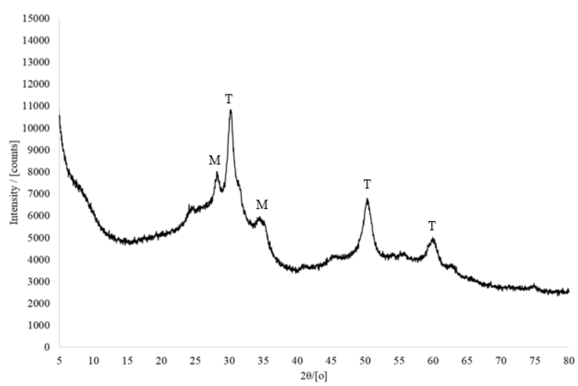

Figure 3: X-ray diffraction spectra of SZ (T = tetragonal crystal and M = monoclinic crystal)

Surface area was obtained by N_2 physisorption isotherms determined at 77K using a Thermo Scientific Surfer and Brunauer-Emmett-Teller (BET) equation with samples outgassed at 150^{o}C over high vacuum for 12h prior to analysis. SZ had a high surface area (277$\pm$15m^2/g), which was twice higher than those reported, i.e. 108m^2/g [43], 119.3m^2/g [47]. The difference could be due to the conditions used during the catalyst preparation. Hamouda et al.[48] and Stichert and Schüth [49] found that the surface area could dramatically vary from 19m^2/g (no aging) to 104m^2/g (1 day aging at 423K) [49].

2.3. Kinetic parameters

Only PET waste were cut into circular particles of 1mm diameter and analysed by thermogravimetric analysis (TGA) in a Perkin Elmer STA6000 at 5, 10, 20 and 40^{o}C/min between 30-700^{o}C to obtain kinetic parameters of PET pyrolysis using isoconversional methods as described in detail elsewhere [50]. TGA and differential TGA curves of the PET waste sample and its kinetic parameters (activation energy, pre-exponential factor and order of reaction) are illustrated in Figure 4 and Table 2 respectively. Figure 5 shows the variation of the waste PET heat flow during TGA analysis as temperature increased.

Table 2: Results of kinetic analysis [50]

	PET waste
Decomposition temperature range / [^{o}C]	395-520
Activation energy / [kJ/mol]	197.61
Order of reaction	2.8

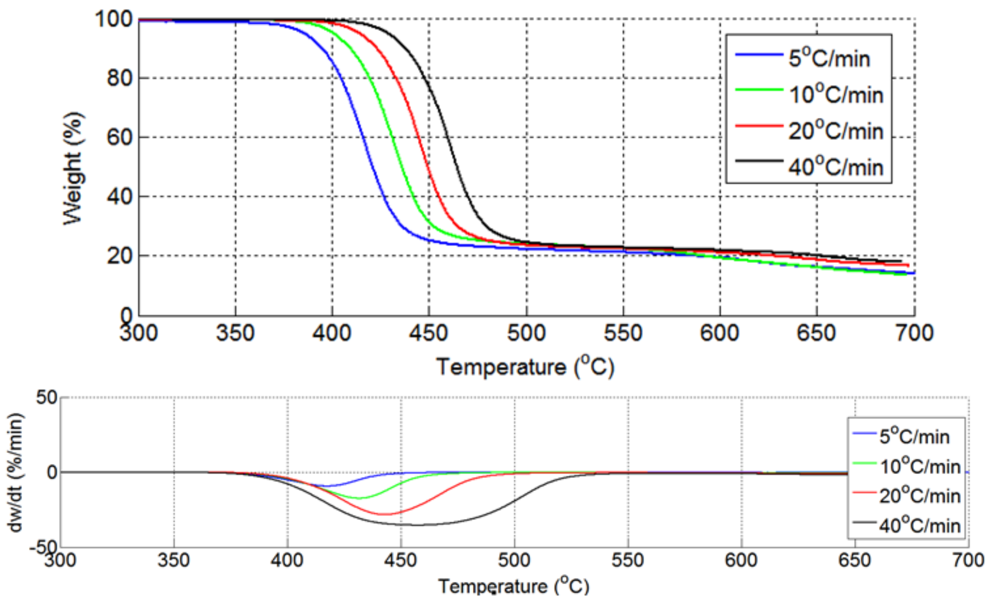

Figure 4: TGA (top) and differential TGA (bottom) curves for PET samples obtain at 5^{o}C/min, 10^{o}C/min, 20^{o}C/min and 40^{o}C/min between 300-700^{o}C

From TGA analysis (Figure 4), it can be observed that PET decomposition started at around 395 ^{o}C and completed about 520 ^{o}C. Figure 5 shows a perturbation on the heat flow after PET decomposition temperature at high heating rates ($>$ 20 ^{o}C/min) that is not perceptible at low heating rates ($<$ 20 ^{o}C/min). This perturbation is thought to be caused by a temperature profile formed on the plastic particle caused by a decrease in the uniformity of the heat distribution at high heating rates due to the low thermal conductivity of plastics. This phenomenon prevents the PET particle to melt completely and therefore part of the thermal decomposition occurs on melted plastic i.e. liquid and part on the non-melted plastic i.e. solid. Pyrolysis temperature for the experiments was set based on the range determined by TGA. The minimum temperature selected was 450 ^{o}C to ensure over 20% PET decomposition. The maximum experimental temperature selected was 600 ^{o}C to obtain complete PET decomposition. The remaining experimental temperature was

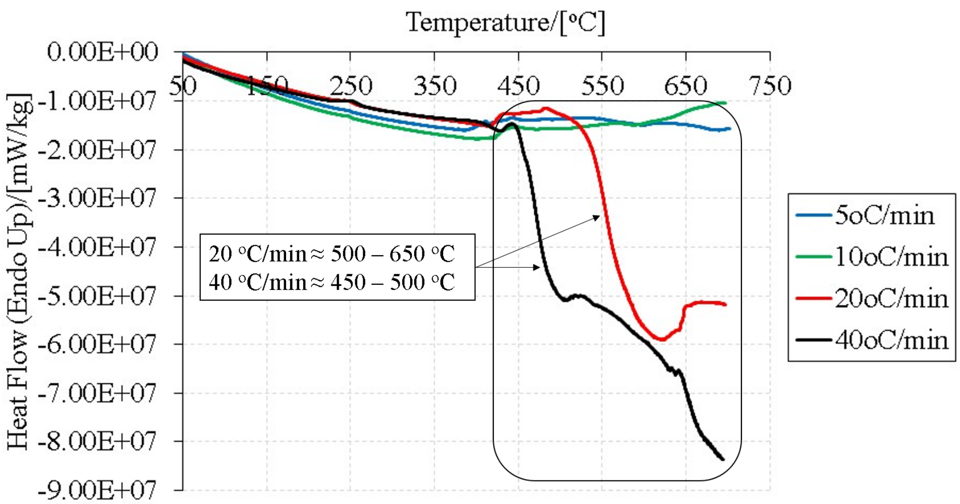

Figure 5: Heat flow (mW/kg) curves for PET samples obtain at 5^{o}C/min, 10^{o}C/min, 20^{o}C/min and 40^{o}C/min between 50-700^{o}C

selected as the medium point of the selected interval.

2.4. Pyrolysis methodology

Experimental set up for pyrolysis was shown in Figure 6. Approximately 5.04±0.03 g of PET were placed in a quartz combustion boat inside a 30 cm long and 29 mm inner diameter quartz reactor. A 10 mm long catalyst bed was created just after the sample by mixing the desired amount of the SZ catalyst (3wt%, 6.5wt% or 10wt% of the PET sample) with 10 g of 1 mm diameter glass beads (Sigma-Aldrich) in order to: i) obtain uniform distribution of the catalyst, ii) ensure uniform contact of the volatiles released from pyrolysis and the catalyst and iii) prevent the catalyst to flow out of the reactor with the volatiles to prevent wax contamination in the condenser.

The pyrolysis reactor containing the PET sample and the catalyst packed bed was placed inside a cylindrical horizontal Vecstar VCTF/SP furnace. The reactor was continuously purged with nitrogen at a flow rate of 20 mL/min for 1 h. As soon as the system was air free (confirmed by gas chromatography analysis of the gas collected at the outlet), the furnace was switched on to heat the reactor to the desired pyrolysis temperature (450, 525 or 600 ^{o}C) at 45 ^{o}C/min. Both the sample and the catalyst bed were heated at the same heating rate i.e. 45 ^{o}C/min up to the same final temperature i.e. 450, 525 or 600 ^{o}C as the furnace heated zone has an uniform horizontal temperature distribution. All temperatures given referred to the one measured at the centre of the heated zone. The heating rate given also refers to the one measured at the centre of the heating zone during the furnace calibration prior to any experiment. The temperature was held for 10 minutes from the time the sample reached its set point before the furnace was turned off to ensure full decomposition of the volatiles released. The residence time of the volatiles inside the heated zone i.e.

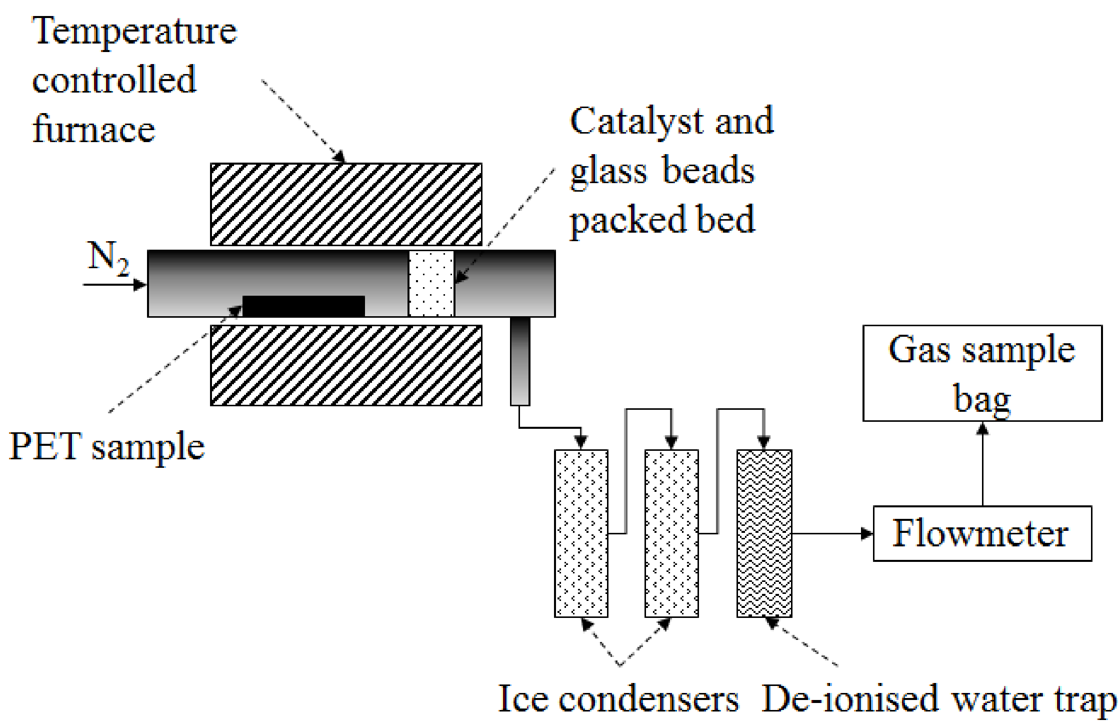

Figure 6: Experimental set up

the time the volatiles remained inside the catalyst bed in contact with the catalyst, was varied (10, 20 or 30 s) by altering the nitrogen flow rate (40 mL/min, 20 mL/min and 13 mL/min respectively).

At the outlet of the reactor, volatiles were condensed in two condensers cooled with ice (0^{o}C). The gases out of the condenser (non-condensable gases) were passed through a water trap to ensure no residues enter the gas collection system. A 0.6L Tedlar bag (Sigma-Aldrich) was used to collect the gas when the sample reached the final pyrolysis temperature (450^{o}C, 525^{o}C or 600^{o}C) for further analysis. The solid residue in the combustion boat and condensed fraction were collected and weighted for their yields once the system cooled down below 100^{o}C under N_2 atmosphere to minimise further decomposition of the products. The gas yield was calculated by mass balance difference as explained in equation 1. The catalyst was recovered from the catalyst bed by simple separation from the glass beads via agitation.

$$M_{PET} = M_{SolidResidue} + M_{Wax} + M_{Gas} \quad (1)$$

where M_{PET} is the initial mass of PET (g), $M_{SolidResidue}$ is the mass of solid residue in the combustion boat (g), M_{Wax} is the mass of the condensed fraction i.e. wax (g), and M_{Gas} is the mass of the non-condensable fraction i.e. gas calculated by difference (g).

The yield of the three products recovered from PET pyrolysis i.e. solid residue, wax and gas, were calculated based on the ratio between the mass recovered and the initial mass of PET, as described in equation 2.

$$Y_i = \frac{M_i}{M_{PET}} * 100 \qquad (2)$$

where i represents the products: solid residue, wax and gas, Y_i is the yield (wt%), M_i the mass of product at the end of pyrolysis (g) calculated either by weighting as explained above or by difference and M_{PET} is the initial mass of PET (g).

2.5. Product analysis

2.5.1. Gas analysis.

Gas samples were analysed by a Varian 450 gas chromatography unit equipped with (i) a TCD detector (held at 175^{o}C) and three columns: Haysep T ultimetal 0.5m x 0.3175mm, Haysep Q ultimetal 0.5m x 0.3175mm and Molsieve ultimetal 1.5m x 0.3175mm kept isothermally in an oven at 175^{o}C and (ii) an FID detector (held at 250^{o}C) coupled with a CP-Sil 5CB 25m x 0.25mm x 0.40μm in an oven programmed as follows: 40^{o}C hold for 2min, 4^{o}C/min to 50^{o}C and hold for 0.5min, 8^{o}C/min to 100^{o}C and final ramp to 120^{o}C at 10^{o}C/min. The results from GC-TCD/FID gas analysis are referred to the initial PET sample (i.e. mass of compound/mass of PET sample).

2.5.2. Wax analysis.

A known fraction of the wax sample was dissolved in n-hexane and analysed by both gas chromatography mass spectrometry (GC-MS) for qualitative analysis and gas chromatography flame ionized detector (GC-FID) for quantitative analysis. GC-MS analysis was performed in a Clarus 560D equipped with Elite-5MS 30m x 0.25mm x 0.25mm column. GC-FID analysis of the wax sample was made on an Agilent 7820N unit equipped with a CPSil5 CB 25m x 0.25mm x 0.40mm column. The method used for both GC-MS and GC-FID was as follows: temperature of the detector and inlet set at 280^{o}oC and oven programmed to start at 60^{o}C with 3min hold and then ramped to 280^{o}C at 6.5^{o}C/min followed by a 13.5min hold. Quantitative results from GC-FID were obtained based on a calibration curve with benzoic acid (99%, Alfa Aesar) at different concentrations as well as injecting 1μL of methyl heptadecanoate dissolved in n-hexane (500ppm, Sigma Aldrich) with every sample as internal standard. Results from GC-FID wax analysis are calculated based on the initial PET mass (i.e. mass of compound/mass of PET sample).

An equivalent amount of wax was also dissolved in dimethyl sulfoxide (DMSO) and analysed by proton nuclear magnetic resonance (^{1}H-NMR) to cross examine the GC-MS results. ^{1}H-NMR of the sample was conducted in a Bruker Avance III HD 700 NMR Spectrometer operating at 700.13MHz. The spectra were acquired in d6-DMSO at 298K and were referenced to TMS. The number of scans was 256. Finally, the wax as collected from the condensed was scanned from 4000-600cm^{-1o} on an Agilent Cary 630, using KBr as background reference.

3. Results and Discussion

PET is a stiff semi crystalline polymer formed by repetition of the structure shown in Figure 1. When PET is exposed to high temperatures ($\geq$395^{o}C), it decomposes via a random scission of the ester linkage resulting in the formation of a vinyl ester and a carboxyl group (benzoic acid). The vinyl ester undergoes transesterification to form acetaldehyde and other smaller molecules such as CO, CO_2 or ethylene [24, 51]. The rate of PET decomposition and its product distribution depends on the temperature, the amount of catalyst/type of catalyst and the residence time of the volatiles [24].

3.1. Effect of operating conditions on decomposition of PET

Figure 7 shows the variation of temperature and catalyst:plastic mass ratio for the gas yield (left), the wax yield (middle) and residue yield (right). It was found that at the tested operating conditions: temperature (450-600 ^{o}C), volatile residence time in the heated zone (10-30s) and catalyst:plastic mass ratio (3-10wt%), temperature had the strongest effect on the product yield, followed by the catalyst:plastic mass ratio. Increasing temperature enhanced the production of the gas at the expense of wax fraction. At low temperature (i.e. 450 ^{o}C) increasing the catalyst proportion increased the solid residue yield but did not have a clear effect on the gas and wax yield. At high temperature (i.e. 600 ^{o}C), the gas yield maximised whereas the wax yield minimised at catalyst:plastic ratio of 2/30 (i.e. 6.5 wt%). In contrast, the solid residue yield increased with catalyst (12.45 wt% with no catalyst, 13.37 wt% at 3 wt% catalyst and 20.28 wt% at 10 wt% catalyst).

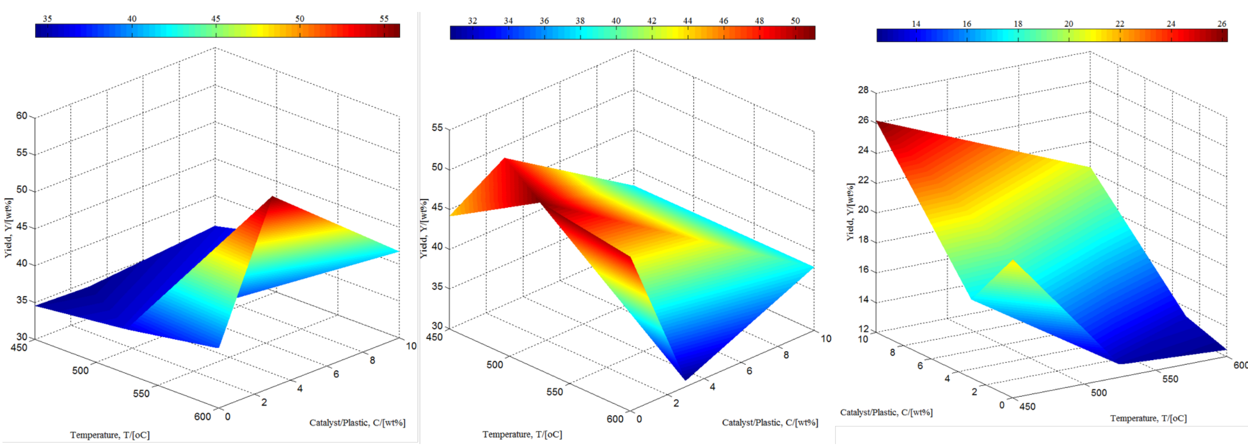

Figure 7: Effect of temperature and catalyst:plastic mass ratio on the gas yield (left), wax yield (middle) and residue yield (right) at volatile residence time of 20s. Red areas represent higher values while blue areas lower values according to the colour bar on top of each subfigure. Green and yellow areas are intermediate values. Errors: gas yield = ± 6.37 wt%, wax yield = ± 7.60 wt% and residue yield = ± 8.53 wt%

As explained in section 2.4, the solid residue represented the residue recovered from the combustion boat after PET pyrolysis. Therefore this fraction was not in contact with the catalyst bed. The solid residue yield varied mainly due to differences in the composition of PET waste i.e. drink bottles, ready-meal packets, etc.

The effect of the catalyst on PET decomposition was more prominent at high temperature (600 ^oC). For example, increasing the catalyst:plastic mass ration at 450 ^oC from 0 to 1:10 (i.e. from 0 wt% to 10 wt%) resulted in a 3 % increase of the gas yield (from 34.54 wt% to 35.87 wt%) while at 600 ^oC the gas yield increased by 29 % (from 38.19 wt% to 55.91 wt%). This suggested the minimum temperature required to activate the catalyst to enhance secondary cracking is above 450 ^oC.

The volatiles residence time i.e. the time the volatiles remained inside the catalyst bed in contact with the catalyst, in the tested range of 10-30 s had little effect the product yields. This observation agreed well with the work by Mastral et al. [52] who observed that the residence time in the range of 0.81-1.45 s had no significant effect on the product distribution of plastic waste pyrolysis at temperatures below 685 ^oC. However, there is a general consensus that longer residence times of the volatiles in the reactor enhance the formation of light hydrocarbons and non-condensable gases due to secondary cracking reactions [32, 53]. Therefore, the little effect of the residence time on the product yields on this study could be due to the small range tested. The residence time could not be altered over a wider range due to experimental restrictions so the effect of reaction-space time was not further studied and will remain constant at 20 s in the discussion from this point forward.

3.2. Effect of operating conditions on the gas composition

As expected, higher temperatures promote the cracking of heavier compounds into lighter molecules, thereby increasing the gas yield and decreasing the wax yield as shown in Figure 7. As reported by Martín-Gullón et al. [30] as temperature increased, a fraction of the already formed residue was further decomposed, thereby increasing the proportion of carbon monoxide and carbon dioxide in the gas fraction. Figure 8 shows the evolution of carbon dioxide and carbon monoxide in the gas fraction with temperature and catalyst:plastic ratio.

It was found that without catalyst, increasing the temperature had little effect on CO_2 yield (19.4 wt% at 450 ^oC to 17.25 wt% at 600 ^oC) while had no effect on the yield of CO (11.5 wt% at 450 ^oC to 11.6 wt% at 600 ^oC). CO_2 yield variation was found to be corresponded to the solid residue yield due to the reverse Boudouard reaction occurring to some extent at the tested conditions to transform CO_2 into CO as shown in reaction (3). At 450 ^oC (theoretical molar fraction: $CO_2 = 0.969$ and $CO = 0.031$ [54]) the forward reaction was promoted towards the formation of CO_2 (Figure 8) and solid residue (Figure 7) whereas increasing temperature to 600 ^oC (theoretical molar fraction: $CO_2 = 0.723$ and $CO = 0.277$ [54]) favoured the formation of CO (Figure 8). Figure 8 initially suggested that SZ could affect the reverse Boudouard reaction to form CO from CO_2 and solid residue. It was reported [55] that alkali and alkaline metals (i.e. Na, Ca, Mg, etc.) decreased the minimum temperature to promote the reverse Boudouard reaction from 700 ^oC to 580 ^oC. It has also been suggested that the surface oxygen in metal oxides like ZrO_2 can act as a substrate for carbon residue deposition via the Boudouard reaction (reaction (3)) at high temperatures [56]. However, no previous work was found involving SZ as a Boudouard reaction catalyst. Therefore, the CO_2 yield reduction at high temperature and high catalyst proportion is suggested to be formed via the

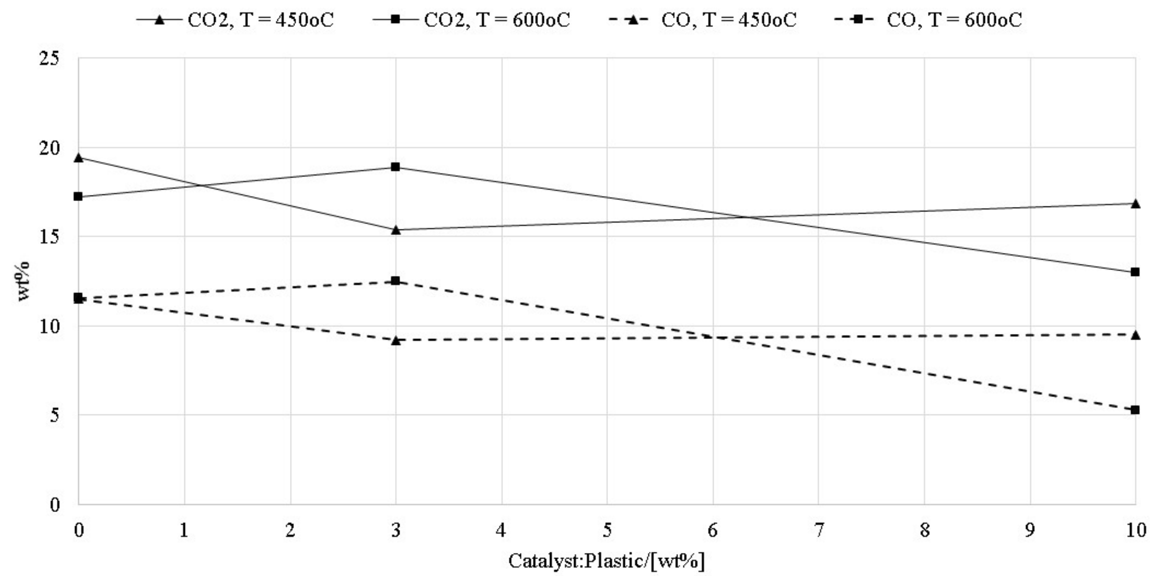

Figure 8: Effect of temperature (450-600 ^{o}C) and catalyst:plastic mass ratio (0-10wt%) on the yield of CO_2 (solid line, $\pm$2.70 wt%) and CO (dashed line, $\pm$1.86 wt%) formation in PET pyrolysis gas. Triangles represent T = 450 ^{o}C and squares represent T = 600 ^{o}C

Boudouard reaction along with carbon residue but consumed by methane in an oxidative coupling with CO_2 as oxidant to form other light hydrocarbons. The carbon residue deposited on SZ surface causes deactivation of the catalyst. Further work on the effect of SZ in the Boudouard reaction will be beneficial to consolidate these conclusions.

$$2CO \leftrightarrow CO_2 + C_{(s)} \tag{3}$$

Figure 9 shows the variation of the remaining gas products: H_2, O_2, CH_4 and C_2-C_5 hydrocarbons with temperature and catalyst:plastic mass ratio at constant volatiles residence time of 20s. The amount of light hydrocarbons (left figure, dashed line, triangles for 450^{o}C and squares for 600^{o}C) increased with both the catalyst:plastic mass ratio (0wt% to 10wt%) and temperature (450 ^{o}C to 600 ^{o}C). At low temperatures (450 ^{o}C) the amount of CO_2 and CO decreased with increasing the catalyst loading (Figure 8), leading to the formation of light hydrocarbons (C_1-C_4) and oxygen (Figure 9). At high temperatures (600 ^{o}C), the formation of CO_2 and CH_4 was favoured at low catalyst loads whereas the formation of light hydrocarbons and oxygen increased with the catalyst load.

SZ catalyst contained crystalline ZrO_2 providing surface oxygen which can interact with some of the reaction products such as CH_4. At high temperature (600 ^{o}C), a proportion of the CH_4 generated can react with CO_2 as an oxidant agent: $2CH_4 + CO_2 \rightarrow CO + C_2H_6 + H_2O$ and $C_2H_6 + CO_2 \rightarrow CO + C_2H_4 + H_2O$ [57, 58]. During this reaction oxygen is necessary to create a methyl radical intermediate (CH_3^*) which can then undergo a chain reaction mechanism to form multiple hydrocarbons i.e. C_2, C_3 and C_4. The oxygen

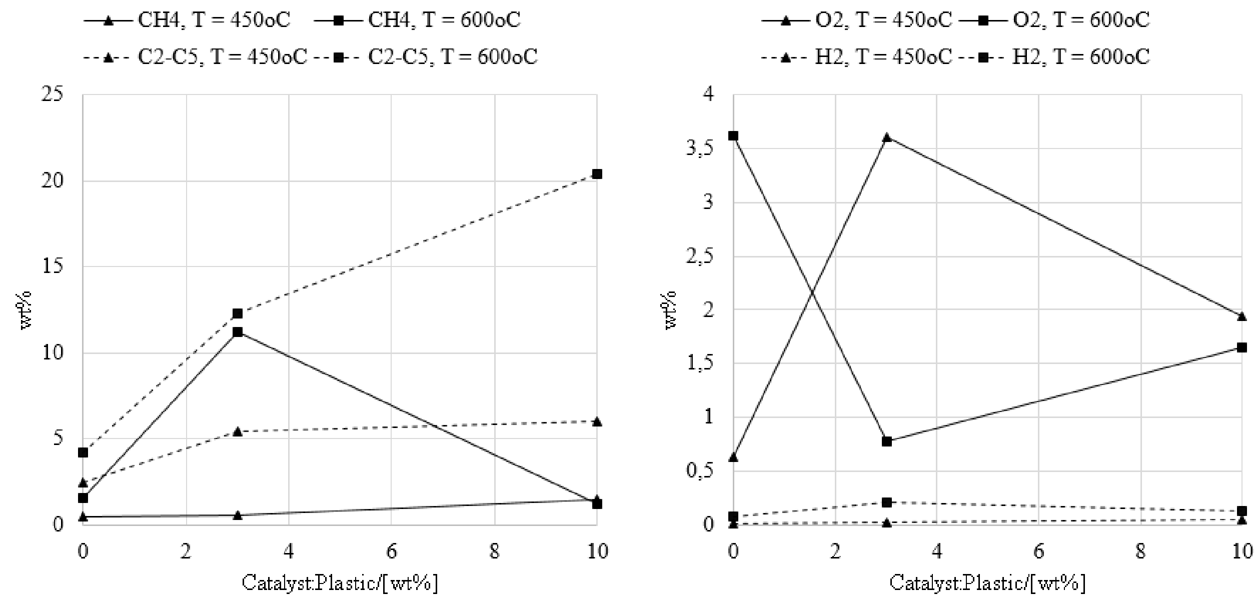

Figure 9: CH_4 (left, solid line, ±1.50 wt%), C_2-(C5) hydrocarbons (left, dashed line, ±2.73 wt%), O_2 (right, solid line, ±1.30 wt%) and H_2 (right, dashed line, ±0.09 wt%) yield (in wt%) at 450 ^oC (triangles) and at 600 ^oC (squares) at 20s residence time and catalyst:plastic mass ratio of 0-10 wt%

in gas phase it can also react with CH_3^* to form further CO_2 via CH_3O_2 and CH_2O radicals mechanism. However, when the oxygen is available at the surface of a catalyst as in this case and not in the gas phase the formation of CO_2 is suppressed and the selectivity of C_2-C_5 hydrocarbons increases [58] explaining the reduction of CH_4 and CO_2 and increase in C_2-C_5 yield at high temperature (600 ^oC) shown in Figure 9.

However, it was found that part of the SO_4 group decomposed into SOx, specially at temperatures above 525 ^oC. TGA analysis of SZ performed by Srinivasan et al. [59] showed two weight loss regions for SZ in helium; an initial 10 wt% weight loss between 100-500 ^oC and a second 6 wt% weight loss between 500-700 ^oC. Therefore for temperatures above 525 ^oC, higher catalyst loads were needed to promote secondary reactions to form light hydrocarbons rather than CO_2 since as the catalyst was decomposed the number of active sites was decreased. Further discussion on SZ thermal decomposition and deactivation is discussed later on in section 3.4.

3.3. Effect of operating conditions on the wax composition

According to ^{1}H-NMR, PET wax was formed by aromatic compounds (peaks mostly appeared within 6.6-8.3ppm region). Shown in Figure 10 is the calculated proportion of aromatic and olefinic fractions presented in the wax obtained by ^{1}H-NMR analysis based on the method proposed by Myers et al. [60].

The olefin content corresponded to the functional groups that are attached to the benzene ring. This confirms the presence of vinyl ester groups in the wax product identified by the GC-MS analysis. The aromatic percentage corresponded to the hydrogen atoms that are attached to the aromatic ring implying that most of the wax product is formed by aromatic compounds as identified by GC-MS analysis. Increasing

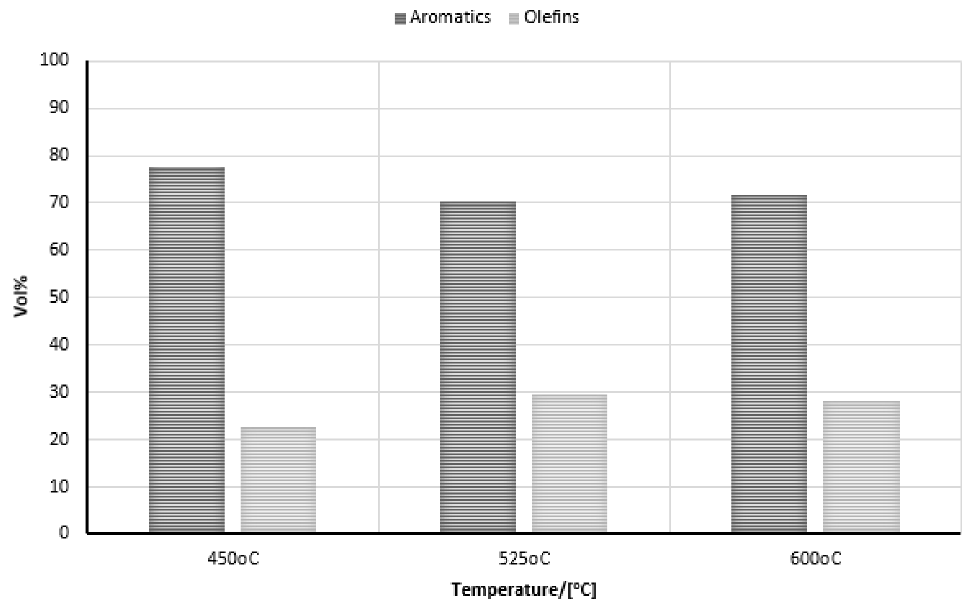

Figure 10: Proportion of aromatic and olefinic fraction in PET wax derived from pyrolysis at 450^{o}C, 525^{o}C and 600^{o}C at 20s volatiles residence time and 6.5wt% catalyst:plastic mass ratio

pyrolysis temperature caused a slight increase in the functional groups at the expense of aromatic content due to further decomposition of the primary compounds as described in Figure 11. However, ^{1}H-NMR results did not show a major difference because they only provide a general composition i.e. aromatic and olefinic, but did not provide information on the individual compounds or functional groups within those two wide fractions. Therefore, the wax was also qualitatively analysed by FT-IR and GC-MS and quantified via GC-FID as shown in sections 3.3.1 and 3.3.2.

3.3.1. Functional groups in PET wax product

The FT-IR analysis of the wax obtained at 450 ^{o}C, 525 ^{o}C and 600 ^{o}C, without catalyst at 20 s residence time are shown in Figure 12. As observed, temperature did not have an effect on the functional groups distribution in the wax fraction except for the presence of two small peaks between 3013-2815 cm^{-1} at 450 ^{o}C which were not present at 525 ^{o}C and 600 ^{o}C. These two peaks corresponding to the C-H stretch in the methylene group (R=CH_2) suggested that as temperature increased the vinyl ester bond decomposes into other compounds. The presence of the most predominant peak at 1730-1630 cm^{-1} related to the C=O stretch and the peak between 1330-1200 cm^{-1} designated to the C-O stretch implies the existence of carboxylic acids (the second peak typically found between 1380-1210 cm^{-1}) or esters (the second peak usually between 1300-1100 cm^{-1}) [61, 62].

The findings from the FT-IR analysis agreed well with those obtained from ^{1}H-NMR and GC-MS with a significant proportion of aromatic compounds (70-80vol%) and olefins (20-30vol%). Peaks around 1000cm^{-1} and 900cm^{-1} corresponded to the C-C and C-H stretch in aromatic rings respectively. These findings confirmed that PET wax was formed mainly by aromatic compounds and therefore it presented a low H/C

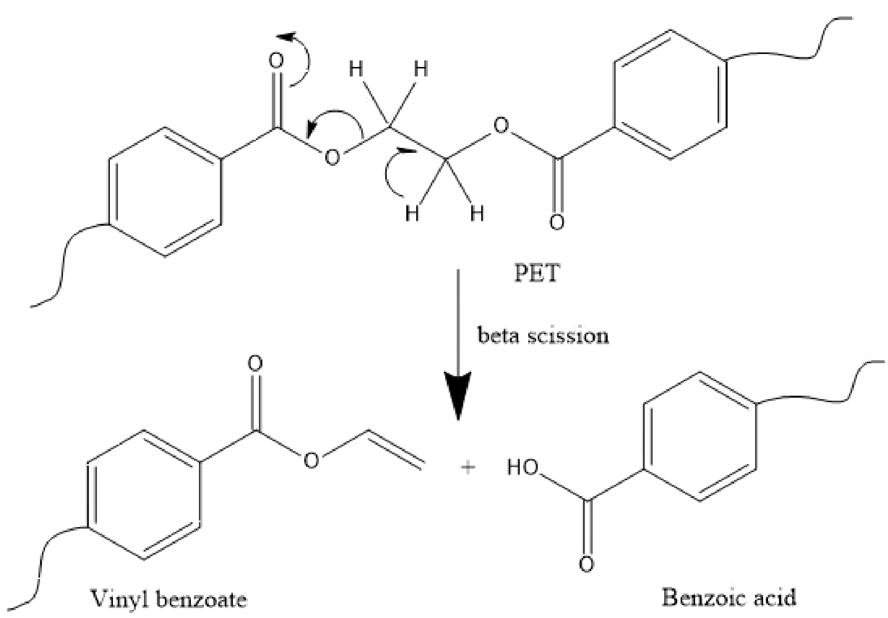

Figure 11: Beta scission mechanism of PET thermal degradation adapted from [24]

ratio as expected. The FT-IR spectrum from PET pyrolysis wax showed in Figure 12 also agrees with previous spectra reported in literature [51].

3.3.2. Wax composition

Based on ^{1}H-NMR and FT-IR results, it can be concluded that the majority of the wax was aromatic compounds. The GC-MS results confirmed that 90-95% of pyrolysis wax comprised of: benzaldehyde, acetophenone, methoxybenzyl alcohol, benzoic ether, benzoic acid and 2-acetylbenzoic acid which agreed well with previous studies [21, 24, 51, 63]. The yields of individual components and the effect of temperature and catalyst:plastic mass ratio on the product distribution are summarised in Figure 3. The GC-FID results showed that the product distribution of PET pyrolysis wax was as follows: 19.02-31.64 wt% of benzoic acid; 1.18-5.88 wt% of acetylbenzoic acid; 0.72-3.22 wt% of benzoic ether; 1.05-2.21 wt% of acetophenone; 0.40-1.22 wt% of styrene; 0.06-0.92 wt% of methoxybenzyl alcohol and the difference by other aromatic compounds (1.82-6.47 wt%) which agrees with composition already suggested in literature [7, 64].

As shown in Figure 11, PET decomposition is initiated (>395 ^{o}C) by beta scission at the carboxylic group where the ester link is broken to form benzoic acid and vinyl benzoate. As temperature keeps increasing the amount of vinyl benzoate formed further decomposes into other aromatic compounds in the wax fraction and lighter compounds in the gas phase. Theoretically, vinyl benzoate undergoes a McLafferty rearrangement yielding acetaldehyde and ethylene [24]. However, acetaldehyde was not found for any of the tested conditions and it is not reported as a product from neither thermal nor catalytic PET pyrolysis in literature [7, 21, 51, 63, 64]. The addition of SZ provides both Brønsted and Lewis acid sites [40]. Lewis acidic sites correspond to the zirconia (Zr) atoms while the Brønsted acidic sites are protons on the surface hydroxyl groups of

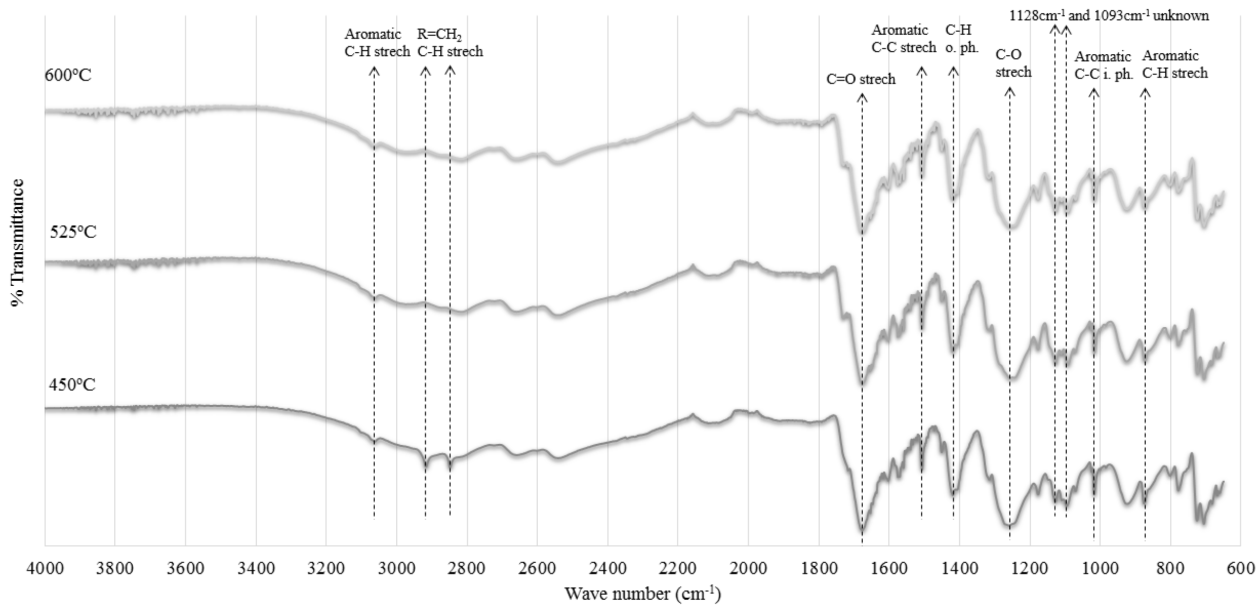

Figure 12: FT-IR spectrums of PET wax obtained at 450^{o}C (bottom), 525^{o}C (middle) and 600^{o}C (top) without catalyst at 20s residence time.

sulfated zirconia oxide as shown in Figure 13. Those active sites promote the formation of carbocations on the surface of the species formed by thermal decomposition via proton donation (Brønsted) or electron acceptance (Lewis) creating active species that further crack into smaller molecules.

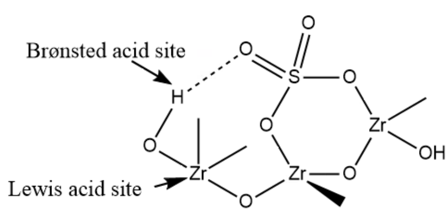

Figure 13: Scheme of the Brønsted and Lewis acid sites on SZ. Adapted from [46]

Temperature and catalyst to plastic mass ratio were the main parameters affecting the formation of benzoic acid (Figure 3). When the temperature increased from 450 ^{o}C to 600 ^{o}C the amount of benzoic acid decreased by 26 % (26.9 wt% to 20.0 wt% ± 1.7 wt%) at 3 wt% catalyst:plastic mass ratio but remained the same (27.4 wt% to 28.0 wt% ± 1.7wt%) at 10 wt% catalyst:plastic mass ratio. At low temperature (450^{o}C) the amount of benzoic acid remain unchangeable (26.9 - 27.5 wt% ± 1.7 wt%) with increasing catalyst:plastic mass ratio from 3 wt% to 10 wt% whereas it was 40 % increase at high temperature i.e. 600 ^{o}C (20.0 wt% to 28.0 wt% ± 1.7 wt%).

Table 3: Variation of PET catalytic pyrolysis wax with temperature (450-600 ^oC) and catalyst:plastic (C/P) mass ratio (0-10 wt%) at 20s volatile residence time. Yield of compound $i = Masscompoundi/InitialPETmass$ where the mass of each compound was extracted from GC-FID via internal standard calibration. Legend: (a) Styrene (±0.44 wt%), (b) acetophenone (±0.61 wt%), (c) methoxybenzyl alcohol (±1.13 wt%), (d) benzoic ether (±1.54 wt%), (e) benzoic acid (±2.67 wt%), (f) acetylbenzoic acid (±0.07 wt%) and (g) other unknown aromatics (±4.84 wt%) calculated by difference, T = Temperature/[^oC], VRT = Volatiles residence time/[s], C:P = Catalyst:Platic/[wt%]

		Product/[wt%]						
T	C:P	(a)	(b)	(c)	(d)	(e)	(f)	(g)
450	0	0.59	1.84	0.90	1.36	27.13	1.66	1.82
	3	1.00	2.21	0.88	3.15	27.53	2.93	3.71
	10	0.40	1.05	0.04	0.99	25.24	1.18	2.69
525	0	0.79	1.21	0.06	2.73	23.91	1.95	3.62
600	0	1.22	2.10	0.08	3.22	31.64	5.88	5.21
	3	0.48	1.60	0.92	1.75	19.02	2.81	4.15
	10	0.45	1.10	0.45	0.72	25.91	2.86	6.47

3.4. Sulfated zirconia thermal decomposition and deactivation

During this study it was found that the SZ catalyst was deactivated due to coke deposition and was partially decomposed at temperatures above 525 ^oC i.e. the weight of SZ after pyrolysis recovered from the catalyst bed was lower than the initial load. The latter explained the low benzoic acid yield at 600 ^oC and catalyst:plastic mass ratio of 1/30 (i.e. 3 wt%) compared to the equivalent at 450 ^oC as shown in Table 3. To understand the behaviour of SZ under high temperature, SZ catalyst thermal transitions were studied in a TA Instruments Q20 differential scanning calorimeter at 5 ^oC/min from 30 - 550 ^oC. Four exothermic peaks were found at: 82.58, 177.43, 455.53 and 525.17 ^oC. The first two peaks (between 80-180 ^oC) were caused by the loss of hydrated water molecules from the zirconium sulphate hydrate ($ZrSO_{42}\cdot xH_2O$) according to the following reaction: $Zr(SO_4)_2 \cdot x\mathrm{H_2O} \rightarrow Zr(SO_4)_2 \cdot y\mathrm{H_2O}$ where y<x. The third and fourth endothermic peaks (between 455 and 525 ^oC) were either caused by the crystallisation of tetragonal ZrO_2 according to: $Zr(SO_4)_2 \rightarrow \mathrm{ZrO_2} + gases$ or by the decomposition of the sulphate into SO_x gases and O_2. This decomposition was previously reported to occur at temperatures above 700 ^oC [65]. Despite Wang et al. [66] suggestion that under N_2 the sulphur content of SZ decreases at temperatures above 500 ^oC, possibly explaining the peak obtained at 525.17 °C, no sulphur compounds were found were detected during experiments at any temperature in neither the gas not the wax fraction. Therefore, the SZ weight loss observed after pyrolysis at high temperature is caused by the loss of hydrated water along with the crystallisation of tetragonal ZrO_2.

SZ deactivation was reported due to either the reduction of the surface sulphate groups from S^{+6} to lower oxidation states at temperatures above 400 ^oC, decreasing both the acidity and activity of the catalyst or due to pore clogging via formation of coke during reaction [67]. SZ deactivation was further studied for another decomposition process of plastic waste [68]. SZ and zeolite HY were both re-used up to four consecutive plastic waste pyrolysis cycles before they showed similar yields than thermal pyrolysis i.e. deactivation of the catalyst caused by coke deposition in the catalyst pores. Deactivated zeolite HY was partially recovered in a parallel work by heating up to 600 ^oC in a CO_2 atmosphere. Up to 77 % of the carbon was removed and the catalyst recovered catalyst performed in a similar way as to spent catalyst after two cycles. Therefore, SZ deactivation due to coke formation could be also recovered by the method mentioned above.

Despite the SZ partial decomposition, SZ has advantages as a catalyst in terms of cost and environmental impact compared to other commercial catalyst such as zeolites, even though it may not be suitable for PET pyrolysis at high temperatures (600 ^oC). When combining catalyst and thermal pyrolysis at 450 ^oC, the yield of benzoic acid was up to 27.0 $\pm$ 1.7 wt% and partial decomposition of the catalyst due to temperature was not observed. This yield was comparable with the one obtained at higher temperatures (20.0 $\pm$ 1.7 wt% at 525 ^oC and 10 wt% catalyst and 28.0 $\pm$ 1.7 wt% at 600 ^oC and 10 wt% catalyst).

Unlike PET glycolysis where the catalyst is commonly in a liquid form that needs to be separated from the products and cannot be reused, SZ is a solid catalyst that is placed on a separate bed and therefore not mixed with pyrolysis products. SZ deactivation was caused by coke deposition and therefore is reversible through regeneration by combustion at 450 ^oC [69, 70] or treatment with hydrogen [71], allowing the reutilization of the catalyst. From previous studies [68], SZ could also be used for several pyrolysis cycles before complete deactivation which then be regenerated for further used without losing its activity. Therefore, the use of this catalyst showed some enhancement over conventional PET pyrolysis and could be considered as an alternative catalyst for low temperature PET pyrolysis.

Assuming an average 24 wt% benzoic acid yield recovered from PET waste, potentially about 408 ktons of benzoic acid could be recovered if all PET waste generated were managed by PET pyrolysis. This could suggest a recovery value of almost $1.8 million per year assuming steady PET waste generation as in the UK in 2014 [1]. In addition, PET waste pyrolysis could avoid the disposal of over 600ktons of PET waste in landfills assuming an average plastic waste landfill disposal rate in the UK of 38 wt% (plastic waste landfill disposal rate in the UK in 2014 [1]).

4. Conclusions

PET is one of the most common plastic waste generated everyday all over the world and is mainly used in food packaging applications which suggests a very short life and consequent rapid generation of PET waste. Currently, chemical recycling through glycolysis and landfill are the main approaches for PET waste management in the EU and USA. Pyrolysis is a promising alternative to recover valuable chemicals without extra costs associated with cleaning and segregation of plastic waste like in glycolysis or mechanical recycling. The results showed that both catalyst:plastic mass ratio and temperature play an important role in the production of benzoic acid, a precursor widely used in the food and beverage industry. High temperature (600^oC) and no catalyst increased by 16% the benzoic acid recovery in the wax product compared to the other conditions tested. However, operation at those conditions is energy intensive due to the energy consumption to achieve high temperature since pyrolysis of PET is an endothermic process. The addition of the catalyst increased the amount of another valuable product i.e. light hydrocarbons (C_1-C_4) from 4wt% without catalyst to 20wt% at 10wt% catalyst:plastic ratio. SZ deactivated due to coke deposition on the catalyst surface as well as partially decomposed at high pyrolysis temperatures i.e. $>525^oC$. This phenomena was not observed when pyrolysis was performed at low temperatures. Based on the costs of catalyst and energy (about $1.4/g (anhydrous) SZ versus $0.10/kW-h on average in 2015 in the IEA [72]), results from this study suggest that PET catalytic pyrolysis in the presence of SZ should be carried out at temperatures below 525^oC and catalyst loads below 10wt.% to obtain high yields of benzoic acid and high value of gas products i.e. high proportion of hydrocarbons.

Acknowledgments

PET waste were kindly provided by O'Brien Recycling Solutions (Wallsend, Newcastle upon Tyne, UK). CHN analysis and X-ray diffraction spectra were obtained at Advanced Chemical and Materials Analysis (ACMA) at Newcastle University and we would like to thank Richard Baron and Maggie White who respectively performed those analysis. ^{1}HNMR analysis was conducted at the School of Chemistry, Newcastle University, by Dr Corinne Willis who we thank for her collaboration.

References

[1] Plastic Europe, Plastic - the facts 2014-2015 (November 11/05/2016).
URL http://www.plasticseurope.org/Document/plastics-the-facts-2014.aspx?Page=DOCUMENT&FolID=2

[2] N. Themelis, C. Mussche, 2014 Energy and economic value of municipal solid waste (MSW), including non-recycled plastics (NRP), currently landfilled in the fifty, https://www.americanchemistry.com/Policy/Energy/Energy-Recovery/2014-Update-of-Potential-for-Energy-Recovery-from-Municipal-Solid-Waste-and-Non-Recycled-Plastics.pdf.

[3] (Trucost), J. Raynaud, Valuing Plastics: The Business Case for Measuring, Managing and Disclosing Plastic Use in the Consumer Goods Industry, Technical report, UNEP (2014).
URL www.unep.org/pdf/ValuingPlastic/

[4] Eurostat, Municipal waste (May 30/05/2016).
URL http://ec.europa.eu/eurostat/cache/metadata/en/env_wasmun_esms.htm

[5] Eurostat, Municipal waste landfilled, incinerated, recycled and composted in the eu-27, 1995 to 2014 (May 30/05/2016).
URL http://ec.europa.eu/eurostat/statistics-explained/index.php/File:

Municipal_waste_landfilled,_incinerated,_recycled_and_composted_in_the_EU-27,_1995_to_2014.png#file

[6] L. Bartolome, B. Cho, H. Do, M. Imran, W. Al-Masry, Recent Developments in the Chemical Recycling of PET, INTECH Open Access Publisher, 2012.

[7] S. Du, J. Valla, R. Parnas, G. Bollas, Conversion of polyethylene terephthalate based waste carpet to benzene-rich oils through thermal, catalytic, and catalytic steam pyrolysis, ACS Sustainable Chemistry & Engineering 4 (5) (2016) 2852–2860.

[8] WRAP, Realising the value of recovered plastic - Market Situation Report, Tech. rep., WRAP (2010).

[9] The Telegraph, Plastic waste 'already building up in UK' following China's ban (05/02/2018). URL http://www.telegraph.co.uk/news/2018/01/02/plastic-waste-already-building-uk-following-chinas-ban/

[10] European Commission, Plastic Waste: Ecological and Human Health Impacts, Tech. rep., Science for Environment Policy: DG Environment News Alert Service, accessed 11/05/2017 (2011). URL http://ec.europa.eu/environment/integration/research/newsalert/pdf/IR1_en.pdf

[11] J. Aguado, D. Serrano, G. San Miguel, European trends in the feedstock recycling of plastic wastes, Global Nest J 9 (1) (2007) 12–19.

[12] J. Hopewell, R. Dvorak, E. Kosior, Plastics recycling: challenges and opportunities, Philosophical Transactions of the Royal Society B: Biological Sciences 364 (1526) (2009) 2115–2126.

[13] B. Johnke, R. Hoppaus, E. Lee, B. Irving, T. Martinsen, K. Mareckova, Good Practice Guidance and Uncertainty Management in National Greenhouse Gas Inventories - Emissions from waste incineration, Tech. rep., Intergovernmental Panel on Climate Change - IPCC (2001). URL http://www.ipcc-nggip.iges.or.jp/public/gp/bgp/5_3_Waste_Incineration.pdf

[14] European Commission (EC), , Integrated Pollution Prevention and Control (IPPC) - Reference Document on the Best Available Techniques for Waste Incineration, Tech. rep., European Commission (2006).

[15] A. Buekens, H. Huang, Comparative evaluation of techniques for controlling the formation and emission of chlorinated dioxins/furans in municipal waste incineration, Journal of Hazardous Materials 62 (1) (1998) 1–33.

[16] D. Carta, G. Cao, C. D, Angeli, Chemical recycling of poly(ethylene terephthalate)(PET) by hydrolysis and glycolysis, Environmental Science and Pollution Research 10 (6) (2003) 390–394.

[17] Q. Yue, C. Wang, L. Zhang, Y. Ni, Y. Jin, Glycolysis of poly (ethylene terephthalate)(PET) using basic ionic liquids as catalysts, Polymer degradation and stability 96 (4) (2011) 399–403.

[18] G. Karayannidis, D. Achilias, Chemical recycling of poly(ethylene terephthalate), Macromolecular Materials and Engineering 292 (2) (2007) 128–146.

[19] M. Khoonkari, A. Haghighi, Y. Sefidbakht, K. Shekoohi, A. Ghaderian, Chemical recycling of PET wastes with different catalysts, International Journal of Polymer Science 2015.

[20] D. Paszun, T. Spychaj, Chemical recycling of poly(ethylene terephthalate), Industrial & Engineering Chemistry Research 36 (4) (1997) 1373–1383.

[21] M. Dzięcioł, J. Trzeszczyński, Volatile products of poly (ethylene terephthalate) thermal degradation in nitrogen atmosphere, Journal of Applied Polymer Science 77 (9) (2000) 1894–1901.

[22] S. Kumagai, I. Hasegawa, G. Grause, T. Kameda, T. Yoshioka, Thermal decomposition of individual and mixed plastics in the presence of cao or ca (oh) 2, Journal of Analytical and Applied Pyrolysis 113 (2015) 584–590.

[23] D. Nikles, M. Farahat, New motivation for the depolymerization products derived from poly(ethylene terephthalate)(PET) waste: a review, Macromolecular Materials and Engineering 290 (1) (2005) 13–30.

[24] S. Venkatachalam, A. Kelkar, J. Labde, K. Rao, P. Gharal, S. Nayak, Degradation and Recyclability of Poly (Ethylene Terephthalate), INTECH Open Access Publisher, 2012.

[25] Global Market Insights, Benzoic Acid Market Size, Industry Analysis Report, Regional Outlook (U.S., Germany, UK, Italy, Russia, China, India, Japan, South Korea, Brazil, Mexico, Saudi Arabia, UAE, South Africa), Application Development, Price Trend, Competitive Market Share and Forecast, 2016 - 2023 (January 25/01/2017).
URL `https://www.gminsights.com/industry-analysis/benzoic-acid-market`

[26] C. Loong, Simulation: Optimize the production of benzoic acid by using benzene and acetic anhydride, Universiti Tunku Abdul Rahman, 2011.

[27] A. Garforth, Y. Lin, P. Sharratt, J. Dwyer, Production of hydrocarbons by catalytic degradation of high density polyethylene in a laboratory fluidised-bed reactor, Applied Catalysis A: General 169 (2) (1998) 331–342.

[28] G. Luo, T. Suto, S. Yasu, K. Kato, Catalytic degradation of high density polyethylene and polypropylene into liquid fuel in a powder-particle fluidized bed, Polymer Degradation and Stability 70 (1) (2000) 97–102.

[29] Y. Xue, S. Zhou, R. Brown, A. Kelkar, X. Bai, Fast pyrolysis of biomass and waste plastic in a fluidized bed reactor, Fuel 156 (2015) 40–46.

[30] I. Martın-Gullon, M. Esperanza, R. Font, Kinetic model for the pyrolysis and combustion of poly-(ethylene terephthalate)(PET), Journal of Analytical and Applied Pyrolysis 58 (2001) 635–650.

[31] R. Lin, D. Negelein, R. White, Effects of catalyst acidity and structure on polymer cracking mechanisms, online (1995).
URL https://web.anl.gov/PCS/acsfuel/preprint%20archive/Files/42_4_LAS%20VEGAS_09-97_0982.pdf

[32] S. Sharuddin, F. Abnisa, W. Daud, M. Aroua, A review on pyrolysis of plastic wastes, Energy Conversion and Management 115 (2016) 308–326.

[33] J. Wu, T. Chen, X. Luo, D. Han, Z. Wang, J. Wu, TG/FTIR analysis on co-pyrolysis behavior of PE, PVC and PS, Waste management 34 (3) (2014) 676–682.

[34] O. Cepeliogullar, A. Putun, Utilization of two different types of plastic wastes from daily and industrial life, Journal of Selcuk University Natural and Applied Science (2013) 694–706.

[35] J. Onwudili, N. Insura, P. Williams, Composition of products from the pyrolysis of polyethylene and polystyrene in a closed batch reactor: Effects of temperature and residence time, Journal of Analytical and Applied Pyrolysis 86 (2) (2009) 293–303.

[36] W. Kaminsky, J. Kim, Pyrolysis of mixed plastics into aromatics, Journal of Analytical and Applied Pyrolysis 51 (1-2) (1999) 127–134.

[37] T. Bhaskar, M. Uddin, K. Murai, J. Kaneko, K. Hamano, T. Kusaba, A. Muto, Y. Sakata, Comparison of thermal degradation products from real municipal waste plastic and model mixed plastics, Journal of Analytical and Applied Pyrolysis 70 (2) (2003) 579–587.

[38] R. Lin, R. White, Acid-catalyzed cracking of polystyrene, Journal of applied polymer science 63 (10) (1997) 1287–1298.

[39] J. Chattopadhyay, T. Pathak, R. Srivastava, A. Singh, Catalytic co-pyrolysis of paper biomass and plastic mixtures (HDPE (high density polyethylene), PP (polypropylene) and PET (polyethylene terephthalate)) and product analysis, Energy 103 (2016) 513–521.

[40] R. Srinivasan, R. Keogh, B. Davis, Sulfated zirconia catalysts: Are Brønsted acid sites the source of the activity?, Catalysis letters 36 (1-2) (1996) 51–57.

[41] X. Li, K. Nagaoka, L. Simon, J. Lercher, S. Wrabetz, F. Jentoft, C. Breitkopf, S. Matysik, H. Papp, Interaction between sulfated zirconia and alkanes: prerequisites for active sites-formation and stability of reaction intermediates, Journal of Catalysis 230 (1) (2005) 214–225.

[42] Z. Helwani, M. Othman, N. Aziz, W. Fernando, J. Kim, Technologies for production of biodiesel focusing on green catalytic techniques: a review, Fuel Processing Technology 90 (12) (2009) 1502–1514.

[43] E. Eterigho, J. Lee, A. Harvey, Triglyceride cracking for biofuel production using a directly synthesised sulphated zirconia catalyst, Bioresource technology 102 (10) (2011) 6313–6316.

[44] M. Van der Stelt, H. Gerhauser, J. Kiel, K. Ptasinski, Biomass upgrading by torrefaction for the production of biofuels: A review, Biomass and bioenergy 35 (9) (2011) 3748–3762.

[45] E. Eterigho, Development and Application of Heterogeneous Catalysts for Direct Cracking of Triglycerides for Biodiesel Production, Newcastle University, 2012.

[46] L. Wang, F. Xiao, Nanoporous catalysts for biomass conversion, Green Chemistry 17 (1) (2015) 24–39.

[47] N. Tangchupong, W. Khaodee, B. Jongsomjit, N. Laosiripojana, P. Praserthdam, S. Assabumrungrat, Effect of calcination temperature on characteristics of sulfated zirconia and its application as catalyst for isosynthesis, Fuel Processing Technology 91 (1) (2010) 121–126.

[48] L. Hamouda, A. Ghorbel, F. Figueras, Study of acidic and catalytic properties of sulfated zirconia prepared by sol-gel process: Influence of preparation conditions, Studies in Surface Science and Catalysis 130 (2000) 971–976.

[49] W. Stichert, F. Schüth, Synthesis of catalytically active high surface area monoclinic sulfated zirconia, Journal of Catalysis 174 (2) (1998) 242–245.

[50] L. Diaz Silvarrey, A. Phan, Kinetic study of municipal plastic waste, International Journal of Hydrogen Energy 41 (37) (2016) 16352–16364.

[51] I. Çit, A. Sınağ, T. Yumak, S. Uçar, Z. Mısırlıoğlu, M. Canel, Comparative pyrolysis of polyolefins (PP and LDPE) and PET, Polymer bulletin 64 (8) (2010) 817–834.

[52] F. Mastral, E. Esperanza, C. Berrueco, M. Juste, J. Ceamanos, Fluidized bed thermal degradation products of HDPE in an inert atmosphere and in air–nitrogen mixtures, Journal of Analytical and Applied Pyrolysis 70 (1) (2003) 1–17.

[53] C. Ludlow-Palafox, H. Chase, Microwave-induced pyrolysis of plastic wastes, Industrial & engineering chemistry research 40 (22) (2001) 4749–4756.

[54] T. Reed, The Boudouard Equilibrium - Gasifiers (12/01/2016).
URL http://gasifiers.bioenergylists.org/files/boudouard_reaction.xls

[55] P. Lahijani, Z. Zainal, M. Mohammadi, A. Mohamed, Conversion of the greenhouse gas CO_2 to the fuel gas co via the boudouard reaction: A review, Renewable and Sustainable Energy Reviews 41 (2015) 615–632.

[56] M. Kogler, E. KoÌĹck, B. KloÌĹtzer, T. Schachinger, W. Wallisch, R. Henn, C. Huck, C. Hejny, S. Penner, High-temperature carbon deposition on oxide surfaces by CO disproportionation, The Journal of Physical Chemistry C 120 (3) (2016) 1795–1807.

[57] B. Eliasson, C. Liu, U. Kogelschatz, Direct conversion of methane and carbon dioxide to higher hydrocarbons using catalytic dielectric-barrier discharges with zeolites, Industrial & Engineering Chemistry Research 39 (5) (2000) 1221–1227.

[58] T. Nishiyama, K. Aika, Mechanism of the oxidative coupling of methane using C_{02} as an oxidant over PbO–MgO, Journal of Catalysis 122 (2) (1990) 346–351.

[59] R. Srinivasan, R. Keogh, D. Milburn, B. Davis, Sulfated zirconia catalysts: Characterization by tga/dta mass spectrometry, Journal of Catalysis 153 (1) (1995) 123–130.

[60] M. Myers Jr, J. Stollsteimer, A. Wims, Determination of hydrocarbon-type distribution and hydrogen/carbon ratio of gasolines by nuclear magnetic resonance spectrometry, Analytical Chemistry 47 (12) (1975) 2010–2015.

[61] P. Larkin, Chapter 7 - General Outline and Strategies for IR and Raman Spectral Interpretation, in: Infrared and Raman Spectroscopy, Elsevier, Oxford, 2011, pp. 117–133.

[62] T. Masuda, Y. Miwa, A. Tamagawa, S. Mukai, K. Hashimoto, Y. Ikeda, Degradation of waste poly(ethylene terephthalate) in a steam atmosphere to recover terephthalic acid and to minimize carbonaceous residue, Polymer degradation and stability 58 (3) (1997) 315–320.

[63] T. Yoshioka, G. Grause, C. Eger, W. Kaminsky, A. Okuwaki, Pyrolysis of poly(ethylene terephthalate) in a fluidised bed plant, Polymer Degradation and Stability 86 (3) (2004) 499 – 504.

[64] E. Dziwiński, J. Iłowska, J. Gniady, Py-GC/MS analyses of poly(ethylene terephthalate) film without and with the presence of tetramethylammonium acetate reagent. Comparative study, Polymer Testing 65 (2018) 111–115.

[65] J. Sohn, D. Lee, Characterization of zirconium sulfate supported on TiO_2 and activity for acid catalysis, Korean Journal of Chemical Engineering 20 (6) (2003) 1030–1036.

[66] P. Wang, J. Zhang, G. Wang, C. Li, C. Yang, Nature of active sites and deactivation mechanism for n-butane isomerization over alumina-promoted sulfated zirconia, Journal of Catalysis 338 (2016) 124–134.

[67] F. Ng, N. Horvát, Sulfur removal from ZrO_2/so_4^{2-} during n-butane isomerization, Applied Catalysis A: General 123 (2) (1995) L197–L203.

[68] L. Diaz-Silvarrey, K. Zhang, A. Phan, Monomer recovery through advanced pyrolysis of waste high density polyethylene (HDPE), Green Chemistry 20 (2018) 1813–1823.

[69] L. Binghui, Deactivation and regeneration of sulfated zirconia, Ph.D. thesis, Tulane University, New Orleans, Luisiana, USA (1998).
URL https://digitallibrary.tulane.edu/islandora/object/tulane%3A24803

[70] C. Li, P. Stair, Ultraviolet raman spectroscopy characterization of sulfated zirconia catalysts: fresh, deactivated and regenerated, Catalysis letters 36 (3) (1996) 119–123.

[71] Y.-C. Yang, H.-S. Weng, Regeneration of coked al-promoted sulfated zirconia catalysts by high pressure hydrogen, Industrial & Engineering Chemistry Research 49 (4) (2010) 1982–1985.

[72] UK Department for Business, Energy & Industrial Strategy, Industrial electricity prices in the IEA (QEP 5.3.1) (January 25/01/2017).
URL `https://www.gov.uk/government/statistical-data-sets/international-industrial-energy-prices`